This article has been accepted for publication in a future issue of this journal, but has not been fully edited. Content may change prior to final publication. Citation information: DOI 10.1109/ACCESS.2019.2928876, IEEE Access

IEEE Access
Multidisciplinary | Rapid Review | Open Access Journal

Date of publication xxxx 00, 0000, date of current version xxxx 00, 0000.

*Digital Object Identifier 10.1109/ACCESS.2017.DOI*

# Underwater Wireless Sensor Networks: A survey on enabling technologies, localization protocols, and Internet of Underwater Things

**MOHAMMED JOUHARI[1], KHALIL IBRAHIMI[2], HAMIDOU TEMBINE[3], AND JALEL BEN-OTHMAN[4]**

[1]Ibn Tofail University, Faculty of Sciences, MISC Laboratory, Kenitra, Morocco (e-mail: mohammed.jouhari@uit.ac.ma)
[2]Ibn Tofail University, Faculty of Sciences, MISC Laboratory, Kenitra, Morocco (e-mail: ibrahimi.khalil@uit.ac.ma)
[3]Learning and Game Theory Laboratory, NewYork University, USA (e-mail: tembine@nyu.edu)
[4]L2S Lab CNRS, centralesupelec, University of Paris 13, France (e-mail: jalel.ben-othman@univ-paris13.fr)

Corresponding author: Mohammed Jouhari (e-mail: mohammed.jouhari@uit.ac.ma).

**ABSTRACT** Underwater communication remains a challenging technology via communication cables and the cost of underwater sensor network deployment is still very high. As an alternative, underwater wireless communication has been proposed and have received more attention in the last decade. Preliminary research indicated that Radio Frequency (RF) and Magneto-Inductive (MI) communication achieve higher data rate in the near field communication. Optical communication achieves good performance when limited to the line-of-sight positioning. Acoustic communication allows long transmission range. However, it suffers from transmission losses and time-varying signal distortion due to its dependency on environmental properties. These latter are salinity, temperature, pressure, depth of transceivers, and the environment geometry. This study is focused on both acoustic and magneto-inductive communications, which are the most used technologies for underwater networking. Such as acoustic communication is employed for applications requiring long communication range while MI is used for real-time communication. Moreover, this paper highlights the trade-off between underwater properties, wireless communication technologies, and communication quality. This can help the researcher community by providing clear insight for further research.

**INDEX TERMS** Underwater Wireless Sensor Networks, Underwater Wireless Communications, Magneto-Inductive Communications, Acoustic Communications, Simultaneous Wireless Power, Information Transfer, Internet of Underwater Things.

## I. INTRODUCTION

Underwater communication remains realized until nowadays via communication cables due to the limited development of underwater wireless communications. However, the use of wires to ensure the connection between sensor nodes at sea bottom results in costly sensor network deployment. For this more intention is given by the researcher community to the Underwater wireless communication. Thus, it is known as a challenging communication medium when it's compared to terrestrial wired or wireless connections. Since a low transmission rate over a short distance is achieved via sophisticated transceivers. Moreover, the marine environment is characterized by several distinguishing features that make it unique and different from the atmosphere environment where the traditional terrestrial communication is performed. As described in the following sections, underwater communication faces several phenomena such as depth related impact on temperature, salinity, pressure, winds, and waves.

Four technologies might be used as an underwater wireless channel. Radio Frequency (RF) employed for terrestrial wireless communication is also enabled for underwater communication; it achieves high data rate for short communication range and suffers from Doppler effect. Optical transmission is also used for the marine environment where the blue-green wavelength is recommended for transmission that requires line-of-sight positioning. Another technology is the magnetic induction that is mostly used for internet of underwater things enabling real-time communication with significant bandwidth since it's independent of the environmental impairment as multipath fading and time-varying signal distortion. However, two issues restrict the use of this technology. Path loss caused by coupling and conductivity between coils. The near-field property due to the non-propagating property of the magnetic wave in the absence of the electric component. The latter technology is acoustic communication, which is the most popular in the underwater communications for its long communication range.

Researchers working on the development of Underwater sensor network should consider a design of a long-term goal that gives a self-configuration ability for distributed sensor nodes within the network [1]. Those nodes are connected through an automatically adaptive wireless link that is capable of automatically fitting with the environmental conditions by changing the system parameters. In some critical applications as a rescue or recovery mission, the network deployment is instant, which does not let time for substantial planning. For this, Underwater Sensor Networks (UWSN) should be capable of configuring itself and managing node location to establish an efficient data communication environment. Also, in case of node failure or channel condition variation, the network should be able to reconfigure itself to maintain its operation.

Typical UWSN is composed of several sensor nodes anchored to the ocean bottom wirelessly interconnected with one or more underwater gateways. Data are usually relayed within this sensor network from the bottom to the sea surface station through multi-hop paths. The underwater gateways are the specific nodes equipped with both vertical and horizontal transceivers. The first one is used to send commands and configuration data to the sensor nodes and get the gathered data from it. The second one is employed to relay the monitored data to the sea surface station. Unlike shallow water, vertical communication is usually required for a long-range in deep water to achieve data delivery toward the surface station. Acoustic and radio modems generally equip this latter. The acoustic communication is used to perform multiple parallel communications to gather data from sensor nodes. Where radio communication usually established with a satellite is employed to relay gathered data to the coastal sink. Differently from [1] where only the ocean bottom sensor nodes are considered and the Autonomous Underwater Vehicles (AUV) to relay data from the bottom to the surface. In [2], Sensor nodes are deployed in different depth to sense the given phenomenon. These sensor nodes use a floating buoy attached even to a surface station or the ocean bottom to keep itself floating at the specific depth. The floating buoy changes its depth, consequently the sensor node with it, by regulating the wire length that relays it to the sea surface or bottom. Although the floating buoys guarantee the easy and quick network deployment, it constitutes a vulnerable aspect of security due to its easy detection on the sea surface.

In the first part, we focused on underwater acoustic communication due to its importance in the deployment of wide-range UWSNs. Firstly we give insight to the underwater acoustic signal propagation which severely depends on the environmental properties such as salinity, temperature, pressure, and depth of transceivers. Absorption and transmission losses formulas are given as well as Channel Impulse Response (CIR). Afterward, time-varying signal distortion is also explained the most relevant papers in the field are cited. By the way, scattering and Doppler effect resulting from transceivers movement or environmental changeability are emphasized. Underwater noises contribute significantly on the acoustic signal impairments where man-generated and natural noise sources are separated and described. Due to the limited energy of sensor nodes, energy efficiency solutions are provided in Section II-C that aims the network lifetime increase. Mobile nodes as Unmanned Underwater Vehicle (UUV) or Autonomous Underwater Vehicle (AUV) are required from wide-range UWSN to cover void region. Additionally, terrestrial GPS does not work well for sensor nodes anchored to the ocean bottom. For this, nodes localization becomes the most challenging issue in UWSN, which is detailed in Section II-D. This study pointed out the major issues facing the physical layer of Underwater Acoustic Sensor Network, which has a strong relationship with the MAC and routing layer. Such as all proposed protocols should deal with the energy efficiency to increase the working time of the network. To this end, the acoustic channel should be considered. As a result, this study helps researchers in the field by collecting and clarifying the different physical issues to develop sophisticated cross-layer protocols.

Afterward, we discuss MI wireless communication, which is an emerging communication method proposed as an alternative for various complicated applications. Such as the Internet of Underwater Things (IoUT) [3], [4], and Wireless Body Area Networks (WBANs) [5]. The preference of using MI communication for those applications is due to the limited interference created between transceivers. UWSN has been considered as a promising sensor network to support the development of IoUT [6]. Which is a novel class of IoT allowed for underwater. It is composed of multiple underwater objects interconnected between each other through MI or another communication medium. Used for monitoring the vast unexplored marine area and enables applications for smart cities development [7]. The acronym IoUT might also describe the Internet of Underground Things [8]. Such as sensor nodes and transceivers are deployed in the underground for monitoring and sensing the target soil area in real time. Recently, application for real-time monitoring of agricultural field has been risen based on IoUT. The main object of this application is to enhance food production through monitoring physical soil parameters such as soil moisture, acidity (pH), organic , and others [8].

UWSN is a heterogeneous network since hybrid acoustic communication system might be used to enhance the network performance [9]. For instance, a combination of the acoustic and optical systems is proposed in [10], [11] to achieve real-

This article has been accepted for publication in a future issue of this journal, but has not been fully edited. Content may change prior to final publication. Citation information: DOI 10.1109/ACCESS.2019.2928876, IEEE Access



**TABLE 1.** Comparison of different underwater communication techniques

| Type | Data rates | Communication ranges | dependency |
|---|---|---|---|
| MI | $\sim Mb/s$ | $10-\breve{\ }100\,m$ | Conductivity |
| EM | $\sim Mb/s$ | $\leq 10\,m$ | Conductivity, multipath Acoustic |
| Optical | $\sim Mb/s$ | $10-\breve{\ }100\,m$ | Light scattering, line of sight communication, ambient light noise |
| Acoustic | $\sim kb/s$ | $\sim km$ | Multipath, Doppler, temperature, pressure, salinity, environmental sound noise |

time video streaming from underwater. Furthermore, IoUT connects heterogeneous underwater objects such as AUVs, anchored underwater sensors, and smart submarine. Additionally, to the fact of heterogeneous, UWSN is known by sparse deployment and mobility of UNs. As a result, UWSN can be considered as Delay Tolerant Network (DTN) [12]. Some recent works give a survey on MI communication [13]–[16], such as [13] provides a comparison of path loss performance of MI, EM, and underwater acoustic communication. Authors in [14] model a broadband channel for underwater MI communication considering the polarization losses of the coil antenna. Thereby a comparison with the existing models is provided. The survey paper [15] of MI communication details the challenges faced in an underground wireless sensor network and [16] gives an overview of various communication techniques perspective for UWSN and the existing algorithms of clustering based on acoustic communication. The paper is organized as follows: Section II gives insight into Acoustic Communications by providing a brief discussing of the acoustic propagation properties and the energy efficiency of UWSNs. As well as describing localization issues. Magneto-Inductive Communication is discussed in Section III by describing the different MI path loss models and reviewing the recently proposed solution to enhance the channel capacity and communication range. Moreover, Simultaneous Wireless Power and Information Transfer (SWPIT) is presented. While the paper is concluded in Section IV.

## II. ACOUSTIC COMMUNICATIONS

### A. ACOUSTIC PROPAGATION

#### 1) Transmission Loss

The underwater acoustic channel (UAC) is known as one of the most challenging communication media actually in use. The acoustic signal traveling between the transmitter and receiver incurs a lot of destructive mechanisms that attenuate received signals. We classified three significant losses types as follows, spreading loss, absorption loss, scattering loss. The later one is discussed separately from this section we firstly introduce the absorption and spreading losses in the transmission loss and attenuation expression. Absorption loss also called viscous absorption, is the energy transfer of the propagating signal into heat due to fluid resistance to flow. Different formulas describing the absorption coefficient are given, we are interested in that considers different oceanic

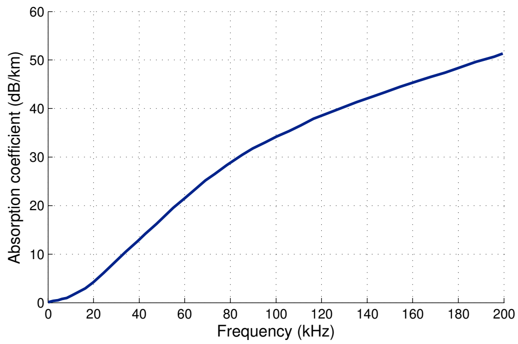


**FIGURE 1.** Absorption coefficient in dB/km.

parameters, such as frequency, temperature, pressure, acidity, and salinity. For frequencies (100 Hz $\leq$ f $\leq$ 1 MHz ) the absorption loss is given as follows:

$$\alpha = \frac{A_1 P_1 f_1 f^2}{f^2 + f_1^2} + \frac{A_2 P_2 f_2 f^2}{f^2 + f_2^2} + A_3 P_3 f^2, \qquad (1)$$

where $f_1$ and $f_2$ (in KHz) are respectively the relaxation frequency of the boric acid and the magnesium sulfate. $A_1$, $A_2$, and $A_3$ are respectively the component in seawater of boric acid, magnesium sulfate and pure water. $P_1$, $P_2$, and $P_3$ are respectively the depth pressure in seawater of boric acid, magnesium sulfate, and pure water. These parameters detail is not the scope of our study, refer to [17] for their formulas. Thorp's formula is used to calculate the absorption coefficient for frequencies above a few hundred Hz as [18]:

$$\alpha = \frac{0.1 f^2}{1 + f^2} + \frac{40 f^2}{4100 + f^2} + 2.75 \times 10^{-4} f^2 + 0.003. \quad (2)$$

The following formula is used to calculate the absorption coefficient for lower frequencies:

$$\alpha = 0.002 + 0.11 \frac{f^2}{1 + f^2} + 0.011 f^2. \qquad (3)$$

Figure 1 shows that the absorption coefficient $\alpha$ increases rapidly with the frequency which restricts the possible maximal frequency to use for an acoustic link with a given distance length. Transmission Loss TL is giving in [17] based on Ray theory, which is the amount of sound intensity decrease such as the received signal is $SL - TL$ Where $SL$ is the sound source signal level. The value of TL caused by the

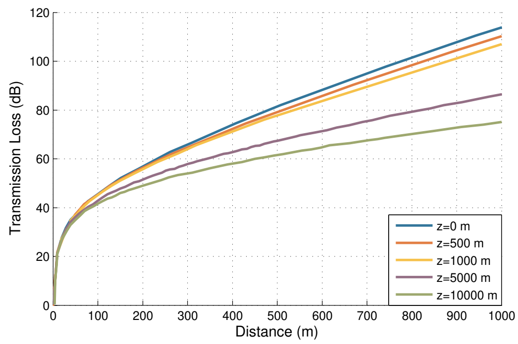


**FIGURE 2.** Transmission Loss versus transmission distance for several depths (z).

spreading loss and absorption is given through the following formula:

$$TL = k \times \log(r) + \alpha r \times 10^{-3}, \quad (4)$$

where k is the spreading factor that depicts the spreading loss in the TL formula, its value depends on the water depth and describes the propagation geometry. In shallow water, $k = 1$ corresponds to cylindrical spreading for deep water $k = 2$ corresponds to spherical spreading. Another case where $k = 1.5$, which is so-called practical spreading, can be considered, it's shown in Figure 2 that transmission loss increases with the depth of transceivers and with the distance between them. Another model is given in [19] to characterize the underwater acoustic channel which is based on the path loss formula that describes the attenuation occurring in a single path over a distance $l$ using signal frequency $f$, it summarizes both spreading and absorption losses. Thus, the overall path loss is calculated by the following expression:

$$A(l, f) = (l/l_r)^k \alpha(f)^{l-l_r}, \quad (5)$$

where $l_r$ is the distance reference. This expression shows the dependency of the acoustic signal attenuation experienced in underwater on the signal frequency and propagation distance.

### 2) Multipath loss

In the last section, we considered that acoustic signal propagates over a single path, which is not the case in the real underwater environment. In underwater the acoustic signal propagates over a long distance is performed through multipath, this is due to the surface and bottom reflection. Although sound refraction resulting from the underwater spatial variability of sound speed, exist only in deep water. Since shallow water is considered as an isovelocity medium due to the constant propagation of sound speed. The latter is strongly dependent on the temperature, salinity, and pressure, which their values vary with depth as shown in the following formula:

$$c = 1412 + 3.21T + 1.19S + 0.0167z, \quad (6)$$

where $S$ is the salinity (in parts/1000), $T$ is the temperature (in $^\circ C$) and $z$ is depth (in $m$). A transmitter sends a beam of rays; each one of them follows a different path and experiencing multiple reflection and refraction during the propagation over underwater. A receiver placed away from the sender receive multipath each one of them has a specific delay and loss. The consideration of multipath losses is important for the development of a sophisticated acoustic channel. The receiver node detects infinite signal echoes due to the long transmission range and multiple reflections and refractions. However, in order to get only the finite number of significant paths, we discard the paths that experienced multiple reflections and lost much energy. To this end, the impulse response of the acoustic channel is used; it depends on the acoustic channel geometry and its reflection and refraction properties. Path delay of $p$th propagation path is calculated by $\tau_p = l_p/c$ where $l_p$ is the $p$th propagation path length which can be calculated using plan geometry. $c$ is the sound speed, we consider propagation in shallow water where sound speed is taken as constant.
The cumulative reflection coefficient is given in [20] is the sum of reflection coefficient undergone by the acoustic signal along a single propagation path, which is denoted by $\Gamma$. Under the ideal conditions, the coefficient of surface reflection equals $-1$ while the coefficient of bottom reflection depends on the bottom type (hard, soft). Based on the cumulative reflection coefficient, the frequency response of $p$th path is given as follows:

$$H_p(f) = \frac{\Gamma_p}{\sqrt{A(l_p, f)}}, \quad (7)$$

Paths of the multipath propagation model act individually as low-pass filter, such as they contribute to the overall impulse response as follows:

$$h(t) = \sum_p h_p(t - \tau_p), \quad (8)$$

where $h_p(t)$ is the inverse Fourier transfer of $H_p(f)$.
Measurements conducted in the Mediterranean shallow waters show that k-mu shadowed distribution outperforms all the classical statistical models [21]. This campaign of measurement is used to get some ultrasonic underwater channel parameters as the channel attenuation, Doppler spread, and the fading statistics. Acoustic signal distortion due to frequency selectivity has not been taken into account by authors since they focused on telemetry applications. The latter does not require a high digital transmission speed. That allows considering the transmission bandwidth as narrow as possible to assume a flat frequency channel (free frequency selectivity). As will be explained in the following section, frequency selectivity might result from multipath losses, and it can be evaluated by estimating the channel response in time and frequency. Underwater acoustic communication systems widely use Low-frequency bands. Hence currently there is a trend of shifting from audio to ultrasonic bands to get the benefits of small wavelength. This is of the interest of

This article has been accepted for publication in a future issue of this journal, but has not been fully edited. Content may change prior to final publication. Citation information: DOI 10.1109/ACCESS.2019.2928876, IEEE Access



UWSN since it allows to transmitter and receiver devices to have more reduced weight and size and operate at lower energy consumption. At the ultrasonic frequencies fading phenomena has a high impact on the channel behavior, which requires precise characterization to design a reliable wireless acoustic communication between the network sensors. Fading or multipath fading is known as the fluctuation of the received signal level resulting from the time variation. This fluctuation may also affect the line of sight (LOS) (Figure 3) component, which referred to as shadowing. Thus, the fading phenomenon is evaluated based on statistical modeling, where each model corresponds to a ray tracing assumption. Such as the main three assumptions considered on the fading modeling are: (1) the existence of a LOS component or not; (2) the deterministic or random behavior of the LOS component; and (3) the possibility of the signal traveling through different clusters of multipath waves. A review of the primary fading model for UAC is given in [21]. Such as the main attribute of these models is their ability to fit the experimental data. Differently from the existing works explained in sub-section that aim the acoustic channel modelization. The attenuation phenomenon of the transmitted signal also appears on the noise level since its distribution in underwater space is non-uniform. That means the noise impact is not similar in the underwater surrounding. This phenomenon appears in the deep water since the majority of noises occur on the sea surface such as the shipping, wind, thermal, and turbulence. The proposed solution in [22] to overcome this problem is to divide the underwater target space into multiple layers regarding the signal strength and noise level in the fading channel and initialize the tree-based multipath.

The authors in [23] show the need for an equalizer to compensate for the time variation of the channel. Where the equalizer implementation requires the knowledge of the propagation channel such as the channel model is useful to reduce the testing time, and it must account for the time variance. Measurements conducted in [23] of underwater acoustic channel time-variant are obtained for a link of 1 $Km$ length. As it's shown, the underwater acoustic channel is doubly spread since the transmitted signal incurs both frequency and time dispersion. The frequency dispersion results from the multipath propagation phenomena and the time dispersion result from the signal scale due to dynamic sea state changes. The scaling time is related to the Mach factor, which is given by $a_p = v/c$ it represents the relative velocity of the transmitter and receiver considering the sound speed. Thus, the channel frequency response is time variant, while the channel impulse response (CIR) is composed of multiple arrival signal paths. Each one is characterized by its amplitude $h_p$ and path delay $\tau_p$. The UAC is considered as wideband since the signal bandwidth is 20$\%$ greater than the carrier frequency. On the receiver side, the time-variant channel amplitude at frequency $f$ is computed as the sum of the arrival $p$ path:

$$H(f,t) = \sum_p h_p e^{j2\pi f \tau_p} e^{-j2\pi a_p(t) f t}, \tag{9}$$

where $h_p e^{j2\pi f \tau_p} e^{-j2\pi a_p(t) f t}$ represents the phase rotation of the received signal at frequency $f$. The use of a long pseudo-random noise (PN) is necessary to extract the CIR in order to ensure a reliable communication system. Although PN is transmitted to maintain a high SNR instead of increasing the transmission power which is limited by the nonlinearity of the front-end, and used to improve the CIR estimation.

Another view of lossy Underwater Acoustic Channel (UAC) shows frequent packet loss during data transmission; thus, a packet level solution is proposed in [24] to improve the transmission reliability. To this end, basic approaches are used, such as the Automatic Repeat Request (ARQ) and Forward Error Correction (FEC). These approaches aim to correct the bit error among the transmitted data packet. The ARQ approach is based on the receiver's feedback, thus resulting in throughput efficiency degradation due to the long propagation delay. In the FEC approach, the bit error rate is detected and corrected using redundant information added to the data packet, which doesn't require feedback. It is recommended for UAC of low bandwidth, long propagation delay, and fast time-varying to use the FEC schemes to correct the bit error. Although FEC is mostly used for UAC, in [25] it's combined with a turbo equalizer whereas combined decision feedback equalizer in [26]. In [24] FEC is adapted and optimized using a fountain-based unicast data transmission scheme to improve transmission reliability over UAC.

### B. DYNAMIC UNDERWATER ACOUSTIC PROPAGATION

#### 1) Time-Varying distortion

The time variability of the UAC channel can be driven principally by two sources: temporal changeability in the propagation environment and motion of transceiver platforms. Environmental conditions resulting in these changes give rise to different time scales signal fluctuations. Some changes occur on a long timescale that has no impact on the communication signals (e.g., seasonal changes in temperature). Others happen in a short timescale that affects the communication signals. The latter changes are induced by the internal waves, turbulent ship wakes, fish migration, eddies, other phenomena, and river outflows. As a result, reflection point displacement engenders signal scattering, and Doppler spread due to path length fluctuation.

The authors in [27], recognize the time-varying multipath arrivals as eigenpath. Where its modulation is composed of two phases for each eigenpath: Time-varying path delay occurring as a result of the transceiver motion due to random waves and current, and time-varying amplitude. Two phenomenas create this latter: transmission loss and fading. Transmission loss phenomenon as described previously it concerns the signal intensity impairment as a consequence of spreading, absorption, and reflection losses [19], [28].

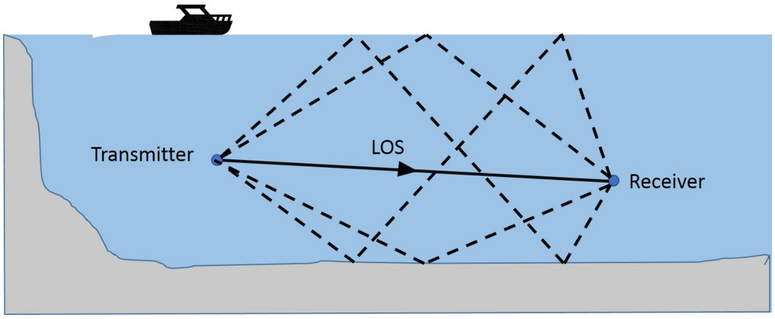


**FIGURE 3.** Underwater acoustic propagation model.

Fading is generally caused by the superposition of multiple transmitted signals within an eigenpath with a different delay [28]. In fact, the received signal can be given as:

$$y(t) = \sum_{p} h_p(t)s(\alpha_p(t - \tau_p(t))), \tag{10}$$

where $h_p(t)$ is the time-varying amplitude, $\tau_p(t)$ is the time-varying delay, and $\alpha_p$ is the time-varying time-scaling factor of the $p$th path. The latter parameter is computed using the $p$th path travel distance $r(t)$ which is divided by the underwater speed of sound propagation:

$$\tau_p(t) = \frac{r_p(t)}{c_w}. \tag{11}$$

The UAC model may designate the propagation channel model as presented in [17], [18] or may denote the mathematical modulation of the channel impulse response [19], [21], [24]. These models are used in underwater channel simulations, networking protocols simulation, or modulation schemes. Although conventional models are developed for narrow-band, its shortcomings are analyzed in [29] through simulation and measurements conducted in a fjord environment. These shortcomings are presented by the frequency-dependent fluctuation rates and frequency-dependent attenuation resulting from the time-varying characteristic precisely from the platform motion. However, it is difficult to model a UAC due to the variety of acoustic channels shown in [30].

The scattering effect that takes part in the propagation losses arises when the transmitted signal is redirected by interacting with a sea object. Sea surface, sea bottom, or the Bubbles may be sources of the scattering phenomenon. Several works have investigated in the scattering caused by the moving sea surface, where two types have distinguished, rough, and calm sea surface [31]. In the case of the smooth sea surface, each scattered path induces a single arrival in impulse response resulting in an inadequate channel impulse response. Contrarily, when the sea surface becomes more dynamic and rough spreading in the delay is joined to the fluctuation in time, resulting in the less sparse impulse response. The impact of scatterers distribution on the Angle-Of-Departure (AOD) and the Angle-Of-Arrival (AOA) is introduced in the stochastic geometry-based channel model developed for wideband Single-Input Single-Output (SISO) UAC [32]. Authors in [32] consider a random distribution of Scatterers and rough condition of the surface and bottom ocean. A new geometry-based channel model raises up [33] for shallow UAC in which slopped ocean bottom is considered. It's shown that even a small slopped bottom has a significant impact on the UACs statistical properties.

Bubbles layer generated by the breaking waves significantly influences the transmitted signals [34] by altering the signal speed, which impacts the transmission loss during the signals propagation and scattering. Contrary to the existing UAC models, the combination of ambient ocean noise and bubble noises is considered in [34]. The rough sea surface is considered in the model [35] using parabolic equation and bubble plume models [36], [37]. Results of [35] show that for strong winds, the impact of bubbles on the transmission loss increase whereas the attenuation of the acoustic signal is dominated by the scattering resulting from bubble plumes rather than sea surface. The author in [38] expanded their model [35] by considering bubble plumes types and found that $\beta$-plumes contribute more in the attenuation than $\alpha$-plumes. Measurement conducted in [39] from near-surface bubbles for the frequency range 1-20 KHz reveals a dependency of frequency, grazing angle, and wind speed in the signal attenuation. It's shown in [40] that for the frequency range 1-4 KHz, the bubbles effect on the sea surface loss is limited to the refraction. While bubbles refraction and extinction jointly contribute to the sea surface loss for the frequency range of 4-8 KHz. Near-surface bubble generated by the wind has an impact on the surface backscattering strength at the frequency 940 Hz [41]. The impact of the bubbles curtain (which is a wall of bubbles Figure 4) on the UWC channel is evaluated in [42]. Transmitted signals passing through this wall undergo significant changes on the signal route and multipath structure. Although, bubbles scattering significantly influences the UnderWater Acoustic (UWA) communication, those resulting from episodic events as a passing ship could be ignored due to its short-term

This article has been accepted for publication in a future issue of this journal, but has not been fully edited. Content may change prior to final publication. Citation information: DOI 10.1109/ACCESS.2019.2928876, IEEE Access



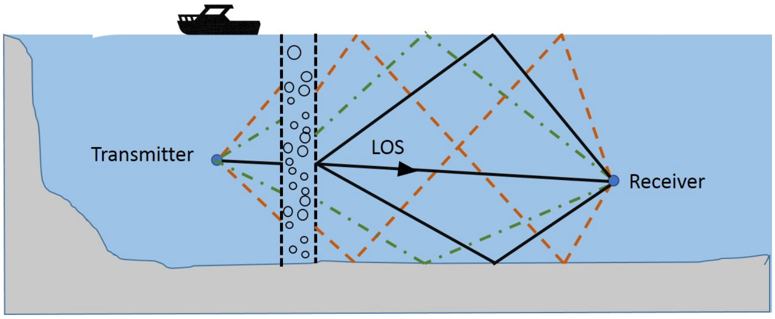


**FIGURE 4.** Example of underwater acoustic communication with bubble curtain.

impact. Persistent bubbles impact is discussed in [43]. This kind of bubbles generated by surface waves could have a benign impact on acoustic communication under a specific wind speed and signal frequencies [44]. Two phenomena principally characterize the UAC: multipath propagation that causes a long time delay and a large Doppler spread [45]. This latter results either from the relative movement of the transmitter/receiver or the propagation medium dynamics [19], [46], [47]. Authors in [45] point out the importance of Doppler effect modelization for UAC and classify the existing models to four categories: the quasi-static model, the uniform Doppler shift model, the basis expansion model, and uniform path speed models, and the recently developed non-uniform path speed model. The Doppler effect appears differently for wideband and narrow-band UWA systems. Due to wideband property Doppler effect influences differently the UAC regarding its frequencies, while is constant for the narrow-band system. A variety of Doppler estimation methods are currently suggested for the UAC to mitigate the impact of Doppler effect on the transmitted signal. Two popular approaches are the most used: the cross-ambiguity function (CAF) and the single-branch autocorrelation (SBA). A multi-branch autocorrelation (MBA) method is proposed in [48] for Doppler estimation in UAC, which can be used in the periodic pilot signals. Doppler phase shift estimator presented in [49] is composed of two estimator phases: coarse and precise estimator, where the estimated value of the precise algorithm is more accurate than the coarse algorithm. The coarse value of Doppler scale effect can be estimated using the Chirp-Z transform (CZT) and compensated by employing the polyphase filter resampling method [50]. Several works propose simultaneous Doppler effect estimation and synchronization [51]–[54], which is an essential task to improve the UWA communication. This task is achieved in [51] by applying two-dimensional auto-correlations to the received signals. Then dual frequency-domain pseudo-random noise is employed as training sequences. Differently, two conjugate Zadoff-Chu (ZC) sequences are used in training sequences to aid in Doppler scaling factor estimation, carrier frequency offsets, and propagation delay estimations [52]. These tasks are accomplished by applying a two-dimensional cross-correlation and two auto-correlation operations on the received signals. While the hyperbolic frequency modulation (HFM) signals are used in [53], [55]. The useless consumption of OFDM bandwidth is avoided by using the central subcarrier as a carrier frequency pilot instead of the additional preamble included in each OFDM frame [54]. In [56] the authors propose a Doppler spectrum model using the summation of the Spike-shape and the Gaussian-shape spectrum components. Such as the first one is used for the Doppler component resulting from the Tx/Rx movement while the second is for Doppler component resulting from the sea surface motion. In order to disable the Doppler effect on the OFDM receiver, a time-varying resampling technique is used in [57] to compensate its impact at each received OFDM frame. A comparison of different methods of Doppler scale estimation using the cyclic-prefixed (CP) or zero-padded (ZP) orthogonal frequency division multiplexing (OFDM) waveforms is given in [58].

#### 2) Underwater acoustic noise

Over the last three decade, oceans have known a continuous increase in human activities in particular shipping traffic that causes significant underwater pollution noise. This noise is crucial on the acoustic channel characterization for underwater communication. Several works have focused on publishing data set and spectral analysis to investigate the impact on the acoustic spectrum. Authors in [59] aim the exploitation of controllable pitch propeller settings and the inherent radiated noise dependencies on the spectral analysis of underwater noise generated by ships. Although narrow-band contributions, broadband noise analysis is investigated in the frequency band ranging from 100 Hz to 4 kHz. Also, different ship classes are considered, such as the fishing vessel, a fishing research vessel, and a merchant ship. The underwater acoustic noise can be distinguished into two categories: site-specific noise and ambient noise [60]. The first category is the noise that depends on geographic localization as those resulting from the breaking ice and sea creatures. The second category includes noises such as turbulence,

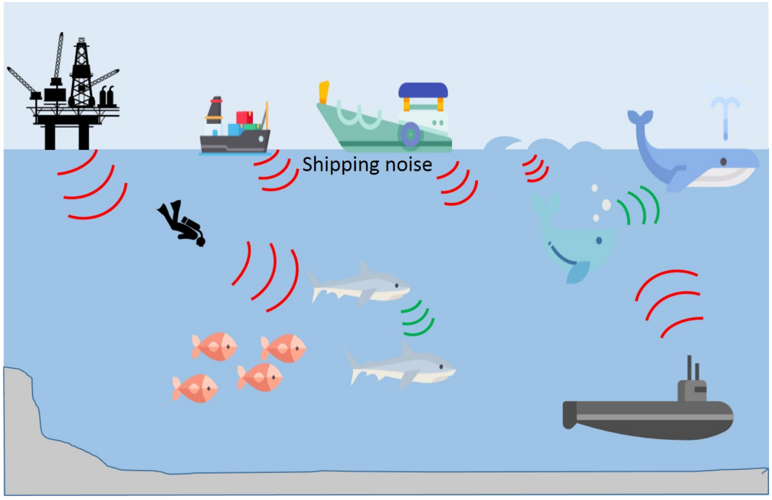


**FIGURE 5.** The impact of man-generated acoustic noise on marine life.

shipping, waves, and thermal.

The statistical characteristics of the acoustic channel strongly influence the performance of underwater communication systems; therefore, most receivers of nowadays consider the Gaussian noise. Since it is the best statistical tool considered in the literature to approximate the cumulative effect of noise resulting from different sources. In that sense, some works [61] found that the noise sources are not always simultaneously contributing to the total channel noise for an operating frequency band. Instead, only one or a few sources dominate the overall probability density function (pdf) [30]. The multiple noise sources existing in shallow water affect the underwater acoustic communication, which makes the use of traditional Gaussian noise models unsuitable. Since receivers designed with such noise model do not perform well at the presence of a non-Gaussian noise on the channel. For this multiple non-Gaussian noise models are suggested, most popular is the Gaussian Mixture (GM) distribution which gets its power from the "universal approximation" properties [62]. Authors in this later provide a detailed analytical analysis of the error performance of an underwater communication system considering GM acoustic channel noise. Rather than assuming the underwater acoustic channel nose as additive white Gaussian Authors in [63] consider colored non-Gaussian channel node. The experimental model, presented in this paper through measurement conducted from different depths in shallow water, shows that power decreases by increasing depth.

Underwater acoustic noise sources are also distinguished by their impact on marine life. Such as two categories are recognized: natural and anthropogenic sources. For natural sources, marine animals already know about their existence in the environment and can easily be adapted to it. Among them, we found sources as waves, rain and seismic, which are characterized by high power and use the same frequency band as marine animals. This might create difficulties in the distance estimation and communication between these animals. The other category is known for its severe impact on the marine animals since it's human-generated, e.g. sonar systems, shipping, and explosions, etc. (Figure 5). Those noises are difficult to distinguish from the natural noises which create accidental collisions between animals and mass beachings. Moreover, animal's behavior is altered due to the latter noise kind, leading them to miss some important noises causing temporary or permanent hearing loss and tissue damage. As a result, studies as [64] have known great interest by the scientific community to investigate the impact of human-generated and natural sounds on marine life, especially marine mammals. To this end, as well as to regulate civilian or military activities as shipping statistical characteristics and spatial distribution of noise sources should be recognized. The process allowing this latter is called profiling, which is achieved through separation, classification, and statistical analysis of noise sources dominating the ambient noises. Noise source profiling has a positive impact on the underwater acoustic communication system, mainly when operating in a harsh environment. Noises and interference occurring in such environment reduce the signal detection performance of the communication system further, the unknown noise distribution makes this problem more difficult to compensate. Authors in [65] employ the Blind Source Separation (BSS) on their proposed scheme entitled Underwater Noise Inspection, Separation, and Classification (UNISeC). This scheme is capable of pre- and post-processing noise analyzes for the three-dimensional underwater multipath environment. It deals with the leak of noise sources information and copes with acoustic contamination through estimating the noise sources as well as their characterization and classifying them using a recursive pilot-aided probing method.

### C. ENERGY EFFICIENCY

Sensors of UWSNs are mostly battery powered, which is characterized by its limited energy, knowing that battery replacement or recharging is not useful in the harsh and far area. For this, saving energy to increase the network lifetime is becoming the principal occupancy of UWSN systems. A variety of solutions are proposed to this end. Delay constrained UWSN is considered in [66] to minimize the energy consumption per bit while preventing retransmissions. Non- coherent binary Frequency-Shift Keying (FSK) modulation and convolutional coding are used to show that the choice of an adequate code rate could decrease the energy consumption per bite while respecting the target maximum frame error rate. Delay-constrained Energy-efficient Routing (DER) scheme is suggested in [67] for UWSN-based communication using the optimization framework based on Mixed Integer Linear Programming, which efficiently computes delay constrained routes for TDMA-based UWSN. DCR find use in time-critical UWSN applications. Although energy efficiency could be achieved by optimizing the end-to-end delay, which is achieved by choosing the minimum hop routing. This solution not necessarily increases the network lifetime due to excessive energy consumption in long links. Thus, efficient energy paths relatively short are chosen for network lifetime maximization that implies the use of high hops number. To cope with this paradox, a trade-off between the network lifetime maximization and the end-to-end delay minimization is proposed in [68] using multi-objective-optimization model. In this sense, it's shown in the study [69] that energy saving is efficiently performed by jointly optimizing the number of hops, retransmissions, code rate, and signal-to-noise ratio for the given link distance. Two scenarios are analyzed with limited or unlimited frame retransmissions for both delay constrained and unconstrained links. This study indicates that for long links, the optimization of the hops-number has a great impact on the energy consumption per bit while is not when increasing the number of allowed retransmission. Refer to Figures 6 and 7 plotted using acoustic channel simulator proposed in [70] by Milica Stojanovic, show respectively one-hop average channel gain impairment and required transmission power as a function of distance. Another way to save energy in UWSNs is to deploy it on cluster mode, where the cluster head is responsible for the fusion and forwarding of coming data from multiple nodes. This method saves energy contrary when each node forward separately its data. The Cluster Head (CH) selection methods could result in more energy saving, thereby increasing the network nodes' lifetime. The CH residual energy and distance by the sink are considered in [71] to determine the candidates' CH in a multi-level hierarchical network. Data aggregation energy efficiency can contribute to extending the UWSN working time. A model designed to this end in [72] developed through the distributed compressed sensing (DCS) theory [73] for cluster-based UWSN. Otherwise, the hot spot appearing during the network communication might reduce its working time [74]. These hot spots are composed of frequently used nodes that quickly drain their energy and die early. This will lead to losing network connectivity, consequently decreasing the network lifetime. To overcome this issue, a cross-layer optimization solution to fairly balance the energy consumption between nodes is suggested in [75], where the link schedule, transmission powers, and transmission rates are jointly optimized. Energy harvesting is a powerful alternative to recharge the battery of UNs, which leads to network lifetime prolongation. This energy can be acquired either from solar, wind, or tidal waves. Otherwise, this technique faces serious challenges that make it sporadic and unpredictable. Thus, battery energy management is a crucial issue to ensure. Authors in [76] suggest a model based on a stochastic dynamic programming approach to optimize the energy allocation for sensing, data collection, and data transmission. This optimization results in allocation policies that ensure the targeted number of successfully delivered packets over a finite-time interval considering both the buffer overflow and the energy capacity constraints. Two channel state knowledge levels are considered as delayed and non-delayed Channel State Information (CSI) feedbacks. Data collection based on the mobile sink (MS) is proposed in

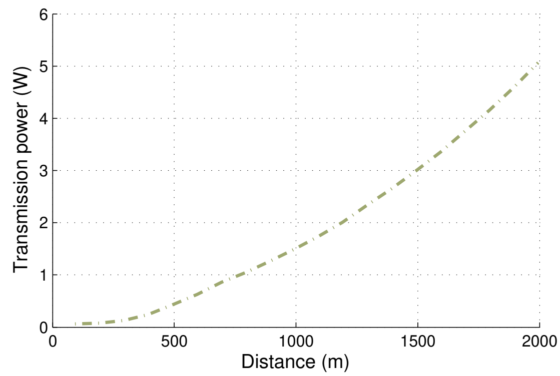


**FIGURE 6.** One-hop acoustic link length versus transmission power.

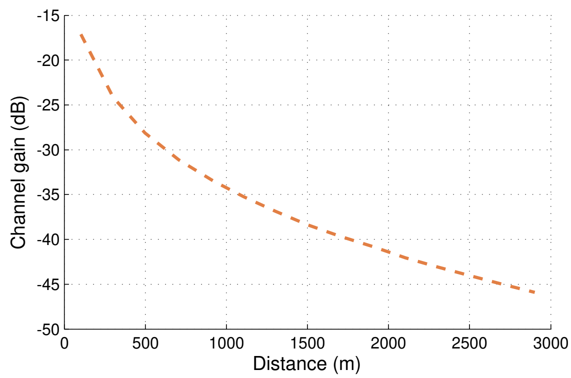


**FIGURE 7.** One-hop acoustic link length versus channel gain.

This article has been accepted for publication in a future issue of this journal, but has not been fully edited. Content may change prior to final publication. Citation information: DOI 10.1109/ACCESS.2019.2928876, IEEE Access



[77] to overcome the problem of the sink neighborhood for network lifetime extension. The sink neighborhood problem also called hot spot problem appears in the static sink-based data collection.

Routing protocols can also optimize energy consumption per bit through choosing the optimal path of the packet to be successfully delivered within an optimal delay, which leads to an increase in the network working time. Some works are proposed in the same sense [78], [79]. In [78] a routing protocol based on energy efficient chain is carried out where the whole underwater area is divided into multiple regions which are assumed as a cluster. The gathered data is communicated between subregion through the cluster head and Relay Nodes (RNs) cooperate with the other nodes to deliver data to the cluster head. To prevent data packet redundancy, a control packet is broadcasted using data stored in CH and RN. Also, the election strategy of the RN is considered. Routing protocol suggested in [79] intended to overcome the energy hols problem through distributing the transmission load among all sensor nodes; it's assumed that all these nodes can control their transmission power to adjust the energy consumed for transmitting or forwarding the gathered data. Indeed, time-varying channel gain characterizing the underwater channel is taken into consideration by this routing protocol. Tow problems of Mobile Sink (MS)-based data collection network lifetime maximization are involved in [80]: the scheduling and routing problem. The first one concerns the determination of the appropriate sojourn time of the MS at specific sink locations for data gathering. The second concerns the use of the optimal path for gathered data transmission that guaranty energy efficiency.

### D. LOCALIZATION IN UWSNS

Potential applications of UWSN require the use of Unmanned Underwater Vehicle (UUV) that gives the mobility aspect of the network to perform well the data gathering task. These vehicles are also known as underwater drone are divided into two categories: Remotely Operated Underwater Vehicles (ROVs) which are controlled from the surface sink or the ship using the remote human operator, and Autonomous Underwater Vehicles (AUVs) which operate autonomously using a predefined set of rules and instructions to navigate in deep water without the need of direct human control. For simplicity, the latter category is called by the underwater mobile nodes which are equipped by acoustic modems for communication and sensors for data gathering. Therefore, mobile nodes need to be accurately localized in order to increase the data gathering accuracy and maintain the knowledge of the whole network topology. The Global Positioning System (GPS) proposed for WSNs does not work well for deep underwater localization due to severe RF Impairments in this environment.

Meanwhile, a GPS system for underwater is proposed in [81] to get the accurate position information of the mobile underwater objects. This system includes GIB (GPS Intelligent Buoys) [82], and PARADIGM [83] which are based on floating buoys acting as their common GPS to provide the absolute position information of the sensor nodes located in their communication range. This localization is obtained based on the distance between nodes given through the Time Difference of Arrival (TDoA) or Time of Arrival (ToA). A target node localization can be obtained by triangulation after estimating its position to the floating buoys. The open issues of UWSN localization attract many researchers. Authors in [84] proposed the use of Kalman Filter for the trajectory estimation, thereby a variety of this filter is investigated to analyze their results. The concerned varieties are presented by the following nonlinear models: Extended Kalman Filter (EKF), Unscented Kalman Filter and Central Difference Kalman Filter. Instead of using the GIB, some localization methods relay on anchors nodes to give the exact location of mobile nodes, where these anchors are underwater nodes fixed at a known position. Kalman filter is used in [85] to align the distances between anchors and mobile nodes based on time-stamp exchanged periodically between them; hence, a time delay is accurately estimated.

The probabilistic graphs concept is emphasized in [86] where all nodes of the network collaborate in such a way to succeed the localization of a target node. For this, a mathematical formulation of the Probabilistic Localization Problem (P-LOC) is calculated through an iterative algorithm that is useful for a lower bound computation on the exact solution. The work in [87] enhances the later algorithm by enabling the run on polynomial time. Where the graph is divided into a special $k - tree$ graph, such as the P-LOC problem can be solved in polynomial time for any fixed $k \geq 1$. Authors in [88] investigate the impact of MAC delay and nodes mobility on the localization accuracy. The MAC delay occurs when anchor nodes communicate between each other through the MAC protocol to avoid packets collision. These anchor nodes knowing their position transmit packets to mobile node aiming its localization. MAC delay joined to the mobility impact can affect localization performance. The study conducted on [88] reveals that the combination of fast node move and longer MAC delay results in a great localization error. To cope with this issue, a localization method combined with multiple access system is proposed. This combination is ensured by enabling the simultaneous transmission to anchor nodes through the use of both frequency division multiple access (FDMA) and hyperbolic frequency modulation (HFM) signal.

The number of anchor nodes is considered in the localization method proposed in [89]. Such as only a few anchor nodes are used to estimate the Euclidean distance between nodes. The location of those nodes is obtained by a weighted least squares method. Although several methods can be used to measure the distance to anchor nodes including the Time of Arrival (ToA), Time Difference of Arrival (TDoA), and the Received Signal Strength Indicator (RSSI), Authors in [89] use the Angle of Arrival (AoA) to estimate the Euclidean distance between sensor and anchor nodes. The proposed method belongs to the category of range-based schemes, where the node location process is divided into three phases: distance estimation, position estimation, and refinement. As it is shown previously, localization is a severe issue for underwater acoustic networks, which is divided into two categories: the self-localization and the source localization. Normally, routing protocols and detection applications perform in function of the self-localization information, such as each sensor nodes are able to get its location individually. A Double Rate Self Localization Algorithm (DRL) is proposed in [90], which reduces required anchor nodes and increases localization accuracy for the multi-hop underwater acoustic network. The DRL scheme is separated into two localization process modes. A low-rate and high-rate transmission mode are suggested to allow the use of the appropriate rate that ensures the transmission rate and increases the measurement accuracy in the network. Furthermore, the influence of references' topology on localization accuracy is reduced using the optimal reference selection algorithm. Although the latter scheme performs well to guarantee a excellent localization accuracy using just one anchor nodes but is limited since only motionless nodes are considered.

Source localization finds use in applications of field exploration including the localization of marine mammals or underwater vehicles. In these applications, the location is estimated through the emitted acoustic signal of target nodes, which is not always certain where comes the need of anchor nodes. Those receivers should be deployed in the underwater bottom to cover a wide area to ensure the target detection and localization, which is not useful in a real scenario. While most of the proposed localization schemes require the use of anchor nodes to estimate the position of a submerged acoustic source [91], authors in [92] proposed an anchorless localization method. In their work, the CIR of the received signal is modeled for multiple possible locations using bathymetry information. The signal can come either from the clicks of dolphins, periodic underwater vehicle pings or marine mammals vocalization. The trajectory of the source node is estimated by comparing the measurement of CIR for each received signal and a database of pre-computed CIR models. The best CIR model location that fits with the measured one is kept in a set of possible node locations; then a trellis form is created from this set to obtain the final source trajectory estimation using a path tracking process similar to the Viterbi algorithm. Instead of accurate sensor node localization, authors in [92] aim to reduce the energy consumption and computational complexity of the localization scheme through reducing the communication between nodes. As the later cited work [92], the scheme presented in [93] is anchor-free. The exact location of the sensor node is calculated by its depth obtained from the attached sensor pressure combined to the two-dimensional information given by the AUV. This later dives into the specific depth to broadcast a packet containing its position using different power levels while moving horizontally. Sensor nodes receive this packet to determine its position; otherwise, sink nodes might take the initiative to estimate the sensor node position, which reduces the computational complexity and increase nodes lifetime.

## III. MAGNETO-INDUCTIVE COMMUNICATIONS

Magnetic Induction (MI) is mostly used for Underground Wireless Communication Networks (UGWN) [94]–[98] where the air is no longer the propagation medium but rock, soil, and water. The feasibility and effectiveness of MI wireless communication technique for the marine environment are demonstrated in [99], [100]. UGWN enable many sophisticated and critical application, including earthquake and landslide forecast, deep sea surveillance and mine wire fare [8], [101]–[103]. Communication over those mediums faces significant challenges such as the path loss, dynamic channel condition, and large antenna size. That is why the communications techniques well established for the terrestrial wireless network are not suitable for the underground wireless network. We take the example of the underwater network, which is the focuses of this study. The propagation over the water is different from the propagation over the air because water has high permeability and electrical conductivity and plane wave highly attenuate in water than in air, this increase rapidly with frequency. MI outperform Acoustic and EM in this point, it performs well without caring about the medium nature (e.g., water or air), it depends only on the conductivity and the magnetic permeability of the medium (Table 1 resumes the difference between MI, EM, and underwater acoustic communications). Table 2 shows magnetic permeability for each medium. Whereas, authors in [13] consider the permeability of the water and air are equal. The propagation delay of MI waves is hugely lower compared to Acoustic waves since MI waves' speed over underwater is about $3.33 \times 10^{-7}$ m/s while is about 1500 m/s for acoustic waves [104]. This property of MI waves could be useful to improve the communication latency and facilitate the development of networking protocols such as the complicated MAC and routing protocols; it will facilitate the design of networking services as localization [105]–[107]. Otherwise, the negligible delay helps on the physical layer synchronization and make it very simple and reliable. Underwater sensor nodes equipped with wire or tuned coil creates a magnetic field that is used to achieve the MI communication between each other. The alternating current passing through the coil attached to the transmitter will induce a current in the receiver's coil. The information is passed through the modulated electric resonant, such as the receiver gets the data information by demodulating the induced current on its attached coil. Conceptually, the source coil could be considered as a magnetic dipole, where its aim, is to maximize the transmission range through creating a maximum field strength, this is achieved by maximizing the magnetic moment.

### A. MI CHANNEL

MI-based communication uses an alternating AC magnetic field as a channel. The difference between the MI signals and the useful electromagnetic (EM) signals in radio communi-

This article has been accepted for publication in a future issue of this journal, but has not been fully edited. Content may change prior to final publication. Citation information: DOI 10.1109/ACCESS.2019.2928876, IEEE Access



| | Magnetic permeability, $\mu\,(H/m)$ | Electric conductivity, $\rho\,(S/m)$ |
|---|---|---|
| Water | $1.256627 \times 10^{-6}$ | 4.80 |
| Air | $1.25663753 \times 10^{-6}$ | $10^{-15}$ to $10^{-9}$ |

**TABLE 2.** Table of conductivity and magnetic permeability over air and water

cation is the neglected component of the electric field that leads to the non-propagating property of MI waves [101]. This is due to the coil resistance radiation that is smaller than the electric dipole used to produce the electromagnetic field since a coil radiates a few energy portions to the far field. Also, the suppressed electric filed could be caused by the involved extremely low frequency (ELF). The non-propagating property is clarified by comparison with radio systems, Where a strong electric field is produced by carrying out a radiation resistance from the electric dipole antenna, more significant than ground losses. In order to circulate the data on the MI carrier modulation techniques as used in radio communication could be considered. The eddy current induced by the magnetic field in the conductive sea water, attenuate and amplify some vector components of the field. This current should be taken into account when designing a transmitter to operate in very shallow water.

Eddy current is a comment problem of both MI and EM communication techniques in underwater networks, it appears on highly conductive underwater medium and causes significant path loss on the transmitted signals. Based on the Faraday's law of induction, the Eddy currents are the electrical current loops induced within the coils resulting from the time-varying of the initial magnetic field. A new magnetic field opposing the changes of the initial field is created by the Eddy current following Lenz's law. On the other hand, the coil antenna performing at high frequencies over a medium of non zero connectivity as sea water will incur high losses. Furthermore, the Eddy current creates a moment opposing the initial moment created by the transmitter that changes the field distribution. The MI signal attenuation is given as follow:

$$\alpha = \frac{1}{\delta} = \sqrt{\pi f \mu \sigma}. \quad (12)$$

A path loss model is developed in [13] considering a dual antenna, its performance analysis is performed through the comparison with acoustic, EM, and the optical channel. This comparison is carried out via the numerical evaluations, where two communication mediums are used, fresh, and seawater. The dual antenna system is composed of two magnetic coupled antennas separated by distance r and is depicted as a two-port network. As an assumption, both antennas are used without losses. In order to ensure the communication range, the transmitted, and received powers given below are essential:

$$P_{TX}(r) = Re(V_1 I_1^*) = Re(Z_{11}) - \frac{Z_{12}^2}{Z_L + Z_{22}}|I_1|^2. \quad (13)$$

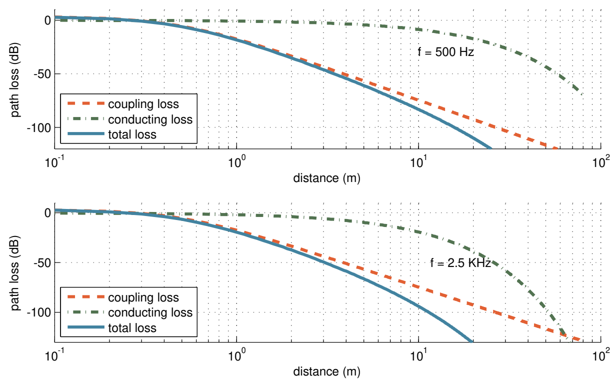


**FIGURE 8.** Path loss vs. distance between two coils for two different operating frequency a) f=500Hz and b) f=2.5KHz.

$$P_{RX}(r) = |I_2|^2 Re(Z_L) = Re(Z_L)\frac{Z_{12}^2}{|Z_L + Z_{22}|^2}|I_1|^2. \quad (14)$$

The path loss (PL) of dual antenna system is defined as following:

$$PL = -10 \log \frac{P_{TX}(r)}{P_{RX}(r_0)}. \quad (15)$$

A time-varying of the magnetic field of the transmitter coil will induce a voltage in the receiver coil resulting from the mutual inductance M. The low frequencies are recommended for the magnetic antenna used in seawater. It enhances the energy harvesting of the MI communication by avoiding Eddy current created by AC magnetic field flux in the transmitter coil. It is clear that the path loss depends on frequency, coil radius, and the number of turns. It decreases by increasing the coil radius or the number of turns and the operating frequency. Dependency between path loss and frequency decrease by using high coil radius. Since the seawater has a high electrical conductivity that induces the creation of Eddy current, the path loss is higher than in fresh water. Based on Equation 15, considering that $P_{Tx}$ and $P_{Rx}$ calculation is different for the given coils and transceivers parameters, Figure 8 shows the total path loss which is the sum of coupling and conduction loss as a function of the distance between coils for different frequencies: a) 500 Hz and b) 2.5 kHz using the scenario in [108]. Normally, numerical results in Figure 8 show that the total path loss increase with distance. Also, it can be seen that at low frequency, the coupling loss is greater than the conduction loss, while it decreases when using high frequency. This means, to increase the communication range, an optimal frequency should be used for the given coil parameters. This issue is frequently discussed in the researcher community of this field [109]–[114].

The magnetic moment is given in [101] in order to boost field strength through the magnetic permeability of the cored coil, $m = \mu NIA$. Where N is the turn number of the loop antenna, I is the current passing through the N turns to create the magnetic field. A is the cross-sectional area of the coil in $m^2$. The moment m could be increased by increasing one of the equation parameters above. However, a trade-off between those parameters arise. The increase of N will induce the increase of copper loss, produce more coupled core loss and the heavier coil will be used as an antenna due to the increase in copper wire mass. The increase of I is followed by the increase of power loss $(I^2r)$ and core loss, such as r is the copper resistance. As a result, a practical drive limit should not be exceeded. Another effective way to increase the moment m, mainly when using coreless coils is by increasing the coil cross-sectional area A. Since m could be increased by a factor of four just by doubling the coil diameter. The modification of the coil geometry (i.e., the length to diameter ratio) results in a massive $\mu$. Consequently, the coil designer should take into account the trade-off between magnetic moment, copper loss, core loss. For 3D grid underwater MI wireless channel [115], performance could be enhanced by choosing the ideal coil radius, inter-coil distance, wire diameter, and capacitance. Theoretical analyses of some network performances are given in this paper, such as SNR, BER, Connectivity, and bandwidth.

Differently from [13] and [115] where authors consider a fixed unidirectional antenna and infinite underwater environment. [116] proposes an underwater channel model to cope with these issues. The marine environment is not always infinite; some applications are developed particularly for shallow water. Then, the designed channel should consider this type of environment and get the benefit of lateral waves. In shallow water, the transmitter coil could be near to the sea surface that results in the creation of a direct path, reflected path, and lateral wave. The last one could enable a long underwater communication range since it experiences less absorption when propagating in the lossless air medium.

Additionally, MI waves traveling from water to air will incur refraction in the sea surface, which is the case in applications performing in shallow water. The refraction is not always negative; it could be positive that is the study scope in [117].

In order to cope with the dynamic rotation of underwater devices, a tridirectional (TD) coil antenna is developed which is composed of three unidirectional (UD) single coils; each one is perpendicular to one of the Cartesian coordination's axes. The software design and hardware implementation are presented in [118], where coils could resonant with the same frequency or three different frequencies. The use of a single carrier frequency facilitates the coil relay deployment that improves communication robustness while the use of three frequencies enhances the multiple access capability.

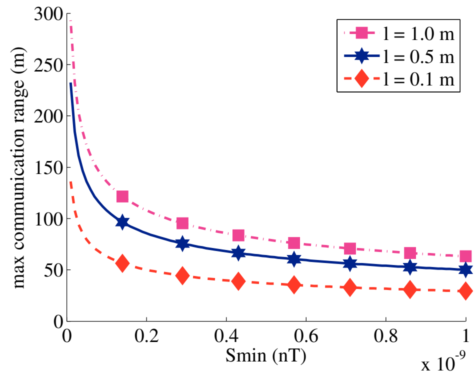


**FIGURE 9.** Maximum distance between two coils versus the minimum detectable signal strength.

The far-field model is developed in [119] based on the magnetic dipole. Magnetic moment and the minimum detectable signal strength $S_{min}$ of the receiver are both used to increase the underwater magnetic field communication range into thousands of meters. Also, the equation of the maximum communication distance is derived as follows:

$$r_{max}^3 = \frac{\mu m}{2\pi S_{min}}. \quad (16)$$

Numerical results presented in Figure 9 given based on Equation 16 shows that the higher is the minimum detectable signal strength, the shorter communication range is allowed. Authors in [120] give a detailed analysis of different path loses occurring in underwater MI link. In addition to path loss described above resulting from coupling loss, a conductive loss is introduced. This is due to seawater conductivity that leads to Eddy current creation. The study aims to find the trade-off between coils design and optimal frequency, considering all power losses in order to establish a coherent link that enables the transmission range of a few hundred meters. This work is released in [108], where a power amplifier is supported by the enhanced quasi-omnidirectional antenna. Then the problems mentioned above and the coupling resulting from the coils misalignment are solved.

### B. PROPOSED SOLUTIONS TO ENHANCE CHANNEL CAPACITY AND TRANSMISSION RANGE

#### 1) Multi-Input Multi-output (MIMO)

Recently, underwater communication has spread out to near-field magnetic induction communication (NFMIC). This technique has some advantages, such as secure communication, less interference, and effective multiple path communication. However, a bottleneck restricts the good use of this technique, that is the degradation of the received signal which decays by the exponential of the inverse sixth power of distance [121]. After it has been studied in RF, authors in [122] proposed MIMO system to improve the communication range of NFMIC. This system has multiple antennas for transmitting and receiving, the number of these antennas

This article has been accepted for publication in a future issue of this journal, but has not been fully edited. Content may change prior to final publication. Citation information: DOI 10.1109/ACCESS.2019.2928876, IEEE Access



increase the communication channels and gives more frequency diversity for the system. In this work, not only MIMO is proposed but also multiple input single output (MISO) and single input multiple outputs (SIMO) are covered by this study. MIMO budget link considered as the distance between the transmitter and receiver is given as follows:

$$\begin{aligned} x &= x' * 10^{\frac{\sum_{\theta=0^\circ}^{\theta=90^\circ} 10\log\left(\frac{\cos^6\theta}{(1+\frac{r^2\cos^2\theta}{x'^2})^3 x^6}\right)}{60}} && \text{if } \theta \text{ different,} \\ x &= x' * 10^{\frac{\sum_{N=1}^{N=n_T+n_R} N*10\log\left(\frac{\cos^6\theta}{(1+\frac{r^2\cos^2\theta}{x'^2})^3 x^6}\right)}{60}} && \text{if } \theta \text{ the same,} \\ x &= x' * \sum_{\theta=0^\circ \| N=1}^{\theta=90^\circ \| N=n_T+n_R} x. \end{aligned}$$

In this equation, the angle variation $\theta$ between the transmitter and the receiver is taken into account. $r$ and $N$ are respectively the radii, and the number of transmitter and receiver, $n_r$ and $n_t$ are respectively the number of transmitter and receiver. As special remarque of this study is recommending for uplink communication to increase the number of transmitters and for downlink communication to increase the number of receivers. The use of multiple conventional antennas in the MIMO system is accompanied by the crosstalk occurred between these arranged circular loops resulting from the inductive coupling. Therefore, MI communication system aiming to increase MI channel capacity employing multi-parallel stream through MIMO system should reduce these crosstalks. Instead of using the same antenna patterns to realize MIMO transmission with limited link capacity. Authors in [123], [124] propose to use a heterogeneous antenna array that enables the crosstalk cancellation. This antenna is composed of a circular loop antenna and the quadrupole loop antenna, which is a double circular loop antenna, as shown in Figure 10. To guarantee the crosstalk cancellation magnetic coupling resulting in this issue should be nullified. In this aim, it ought to nullify the entire magnetic field of the quadrupole loop antenna to create the cancellation plan. By using different current direction in each loop of the quadrupole, we create an opposite magnetic field that cancels each other. Hence, to ensure the free crosstalk transmission transmit antenna should be located on the cancellation plan of the receiver antenna. As it is known the total magnetic field is given in function of the antenna loop parameters as the radius, the number of turns and the distance from its center, so these parameters are used to create the cancellation plan in a specific point.

#### 2) MI waveguide

MI waveguide is a series of relay coil antennas placed between transceivers in order to extend their transmission range. The sinusoidal current passing through the transmitter coil creates a magnetic field that reaches the next relay coil. Consequently, a sinusoidal current is created in this coil that induces a sinusoidal current in the next relay coil and so on until reaching the receiver coil. Thus, the transmission range of transceivers is extended regarding the number of relay coils between them. This technique is discussed in [125], [126] where a passive relay is used to solve two among three major bottlenecks of underground wireless communication such as dynamic channel condition and large antenna size. The passive relay coils are simply coils without processing ability and source of energy.

Authors in [127] proposed to add new functionalities to relay coils in order to improve the performance of waveguide technique. The active relay used in [127] is a series of coils antennas that can process and forward the received signals. Many schemes could be supported by those relay coils. Firstly, the amplification and forwarding scheme denoted as AF. This is the simplest one where the received signal is amplified and forwarded. The amplification is performed through a constant frequency flat. The second scheme, filters after forwards the received signal is denoted by FF. Unlike to AF, FF uses selective frequencies for the signal amplification than a constant frequency flat as AF. The third one is decoding and forwarding called by DF relaying scheme. In this scheme, the linear mapping between the received and transmitted signals has vanished. Additionally, the establishment of full duplex relaying mode is introduced and analyzed.

Multi-hop relaying is proposed in NFMIC [128] for communication range extension and channel capacity enhancement. This technique is based on the network topology where idle nodes deployed in the network are used as cooperative relaying nodes. Three cooperative schemes are studied in this work, where there is no line of sight (NLoS). In the first scheme, only one node is used as a relay. For the remaining two schemes, multiple idle devices are considered with deference in the selection strategy of master and assistant relay that is performed based on the node's location. A 3D analyzes given by N. Ahmed, and all in [129] shows that the use of the spherical configuration of three relaying coils is recommended in the development of multi-coils communication systems. Indeed, the three coils considered in the study are arranged orthogonally in the same center. An extra configuration analyzes provided where the coils are arranged in three different sides of a cube with different coils center.

#### 3) Metamaterial-enhanced magnetic induction $M^2I$ communication mechanism.

The magnetic wave of MI communication system attenuates fastly in a lossy environment as underwater due to many parameters as mentioned above. To overcome this problem, the metamaterial is proposed in [130] to enhance the magnetic field around transceivers that will increase the transmission range. The idea of this technique is that the coil antenna is enclosed by a metamaterial sphere then the magnetic field traveling through the metamaterial layer will increase the MI communication range. The metamaterial sphere is used principally to enhance the near-field range such as its benefit is characterized by the tradeoff between $L_i$ and $M$ through the induction gain that's denoted by $G_m$, which is:

$$G_m = \frac{R_c^0 |M^{meta}|}{(R_c^{meta} + wL_i^{meta})|M^0|}, \tag{17}$$

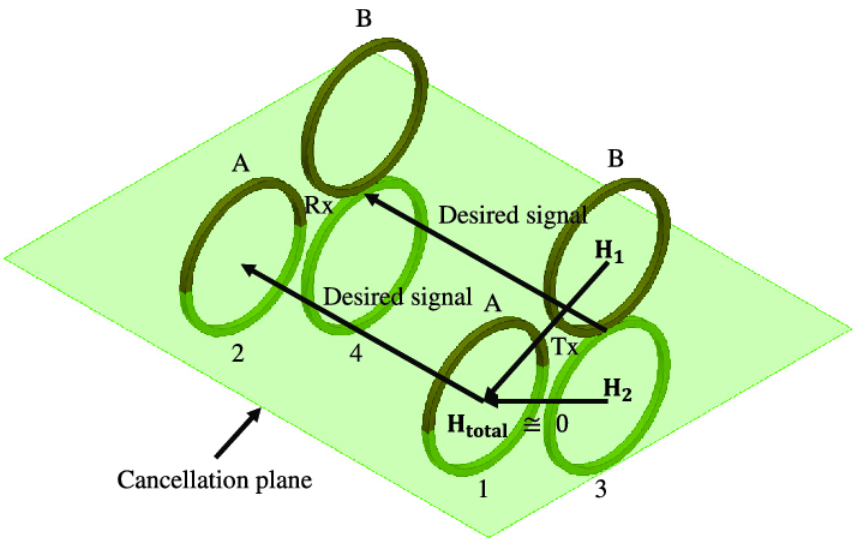


**FIGURE 10.** Heterogeneous multi-pole loop antenna proposed in [124] to enable the crosstalk cancellation plan.

where $M^{meta}$ and $M^0$ are respectively the mutual inductance by using and without the metamaterial sphere. The coil resistance using and without metamaterial are respectively $R_c^{meta}$ and $R_c^0$, $w$ is the angular frequency.The metamaterial has the ability to dramatically change the properties of self-inductance $L$ and mutual inductance $M$. Thus the real component $L$ of the magnetic field becomes a complex number depending on frequencies $L_i$. The model presented in [130] is totally theoretical; thus, the implementation of a real model is a challenging task since there is no instruction on design and the fabrication of the spherical metamaterial. Authors in [131] propose the use of a spherical coil array as spherical metamaterial to realize $M^2I$. This sphere is composed of multiple small coils distributed on a spherical shell that enhance the magnetic field radiation. Consequently, the communication range and data rate are increased. Based on [131] authors propose a prototype [132] using a printed RLC circuit on FR4 substrate as shown in Figure 11. Paper [133] shows the existence of a gap between the real and theoretical prediction in the performance of $M^2I$ based on spherical coil array. This happens even if with efforts engaged in [133] to ensure the optimal condition that achieves the negative permeability in order to extend the radiated field. Not only coil antenna parameters enclosed inside the metamaterial has an impact on the radiated field. However, also the infilling material separating the coil and metamaterial can improve the mutual inductance [134]. A comparison of a small antenna with the previous model [130] showed that a minimum 5m of transmission range is performed.

#### 4) Dynamic freaquency adptation

The best operating frequency where the MI channel perform at its best bandwidth as it is shown in [109] is related to the distance between coils and the deployment arrangement of them. Since the lateral arrangement of a couple of coils prevents the MI communication between them. The underground communication environment (which is the scope of [109]) knows random variation (particularly in soil moisture), where comes the need for dynamic frequency selection, to adopt the best operating frequency selection with the soil condition. Either using the operating frequency the system performs poorly in the presence of the parasitics capacitance. This hidden capacitance appears when a coil is having the inductance $L$ operate without any capacitor in series or parallel. So this parasitic capacitor takes the role of the capacitor C. A soil path attenuation model is developed to get the operating frequency based on soil condition and the communication distance. Differently, in some cases, the dynamic frequency adaptation solution is not good in term of energy harvesting and the robustness challenges, and the proper solution could be obtained just by increasing the number of wire turns. The previous work is followed by [135] of the same authors where a strategic frequency adaptation scheme is proposed for MI-Wireless Underground Sensor Networks according to the medium condition surrounding the MI-nodes.

In this study, a normal medium condition is considered rather than the worst corresponding to high soil moisture. The last case is a strategic and straightforward approach, but it reduces the bandwidth of some applications where the condition is not worst for the majority of the time. This study recommends the use of at least two distinct wirings for each coil to switch between them while seeking the optimal frequency. That allows the optimal MI-communication under different soil condition. An environment-aware method is developed in [136] to better selecting the optimal operating frequency and routing relay in the network. This method is

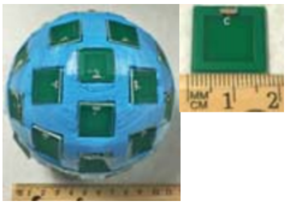

FIGURE 11. 3D printed spherical structure with coil antennas [132].

used to estimate the negative/positive factors of a complex environment based on real training data obtained from the handshaking process between transceivers. That help to predict the environmental impact of the channel to better select the operating frequency.

Consequently, network efficiency is significantly improved. The bandwidth is extended by a factor of three through the dynamic adjustment of the resonant frequency of MI coil [112]. This is due to the transmitter coil equipped with a variable capacitor. Frequency adaptation is also required to improve the connectivity of the MI ad-A Compact Magneto-Inductive Coil Antenna Design for Underwater Communications ad-hoc network [113]. Such as a frequency-switching optimization method is proposed based on the gradient descent algorithm. Moreover, the adequate coverage space of a MI node is obtained by a Lambert W-function based integration.

MIMO technic proposed in the previous section to improve the communication range is presented differently in [110], such as each element in the MIMO array antenna is using its resonant frequency to achieve multiband in order to enlarge the overall bandwidth of the system. The mutual coupling created between those coils due to resonant frequencies diversity is captured and used to get the optimal antenna array configuration that resonant at the expected frequency band to achieve perfectly the multiband. Differently from all the existing MI-waveguide solution proposed above that are proposed to extend the transmission range, where the same resonant frequency is used for all relay coils. The Spread Resonant strategy (SR) used in [111], obtain the optimal solution for all MI relay coils, considering the major MI issues, including the parasitic capacitor appearing in each MI coil, and Eddy current. The SR strategy allocates a different optimal frequency for each MI relay and transceiver coil. The SR frequencies are sufficient to extend MI channel bandwidth and by the way, increase the channel capacity. Further, the path loss is decreased using the optimal central operating frequency.

### C. SIMULTANEOUS WIRELESS POWER AND INFORMATION TRANSFER (SWPIT)

MI knows a growing interest in the realization of applications requiring contactless or Wireless Power Transfer (WPT), due to its high efficiency. Although it is known in the context of near-field communication systems [137], it misses some applications requirement, especially in term of transmission range. To overcome this issue, many solutions are proposed, such as the use of magnetic beamforming or the Magnetic Resonant coupling (MRC). In the Inductive Coupling (IC) technique, a pair of coupled coils are normally used, while the receiving coil located in the radiated field employ the induced current to save power. Most recent researches are focused on the study of the active power transfer [137], [138]. While in [139] authors study the effect of reactive power on the MI system. They found that the ratio of the reactive power on the radiated magnetic field is not related to the power or the current passing through the coils but is related to the geometry of the coils.

Simultaneous Wireless Information and Power Transfer (SWIPT) is recently proposed by S. Kisselef and all in [140]. It combines the WPT and information transmission using the same transmission signal. To this end, the optimization of the power allocation of the transmitter is needed. Since their proposed model is composed of a single transmitter and multiple receivers. The three orthogonal coils antenna described in [129] is used as a transmitter which enables the free self-interference while the receivers deployed randomly around the transmitter use the single coil antenna. In order to satisfy the users' requirement in term of QoS as SNR, two optimizations problems are considered. The first one is the maximization of the received power sum of all power receivers while taking into account the data receiver QoS. The second is the maximization of the received power by the worst receiver while considering the same QoS requirement. The problem of alignment that has a substantial impact on the power transfer is solved in [140] by using the three orthogonal coils antenna. Otherwise, authors in [138] proposed an optimal placement of power transmitter within the target region in order to achieve an efficient power transmission regardless of the power receiver location in this region. WPT use the MRC to expand its transmission range unlike to IC witch use simple transceivers coils. In MRC coils are equipped with an additional capacitance which allows transmitter and receiver to resonant at the same frequency. This ensures an excellent power transfer efficiency over a long transmission range compared to IC. By extending the transmission range, more nodes are covered by the power transmitter where comes the need of networking protocol. Multiple power receivers are located randomly from the transmitter which requires power circuit adaptation to keep them resonant at the same frequency. To this end, an in-band communication protocol is proposed in [141] to manage the network and control the power circuit. Two methods are commonly adopted in [142] to enable WPT based MRC. First one is through resonators, which are tunable RLC circuit placed close to the transceiver coils. It allows the transceivers to resonate at the system's operating frequency, which improves the power transfer efficiency. The second method is based on capacitors of a variable capacity embedded in the electric circuit of the power transmitter and

This article has been accepted for publication in a future issue of this journal, but has not been fully edited. Content may change prior to final publication. Citation information: DOI 10.1109/ACCESS.2019.2928876, IEEE Access



receiver using the operating frequency of the system to ensure resonance. The second method performs the first one due to the additional power loss produced by resonators known by the parasitic resistance [109]. Recently WPT is deployed [143]via a separated way such as two methods are used for data and power transmission. The parasitic capacitance generated by the coupling coils and the metal shield plates is used for data transfer via high frequency, while the magnetic field radiated by the coupling coils is used for power transfer via low frequency. So the power and data are transferred respectively via a magnetic and electric field.

Magnetic beamforming is enabled when multiples TX coils are focusing their magnetic field in a beam toward the target RX coil. This method is applied to enhance the WPT efficiency; its good use requires the optimization of the beam for MRC-WPT [144]. So as the optimization problem is formulated to find the optimal current that should flow through different TX coils since an optimal power is drawn by TXs form their voltage source and the RX load power requirement is minimal. Thereby, this optimization problem requires a complicated computation, especially when more TXs are concerned. To deal with this issue, authors in [145] propose to enable the beamforming scheme with low computation to expand the wireless charging distance. The vision consists of canceling the additional Magnetic coupling between transmitters that reduce the computation complexity to make transmitters and receiver circuit resonate at the same operating frequency by neglecting the phase alignment of transmitters. This is enabled by using the non-coupling coils pattern, as shown above in Figure 10.

SWIPT based MI is mostly used on the Internet of Underwater Things (IoUT) [3], [5], [146], [147] where an enormous number of underwater objects must be connected with each other. Since 2011 MI communications have gained insight from RF, Acoustics, and Optical communication in this field [12]. Such as IoUT applications require some conditions that are satisfied by SWIPT-MI [3] based on novel modulation and demodulation scheme, which is based on the network topology instead of the signal waveform, those requirements are highlighted as follows:

1) *Low hardware complexity*: simple and low-cost transceivers are required which already satisfied with MI transceivers coils for both data and power transfer.
2) *Energy harvesting*: this is enabled efficiently through SWIPT-MI where simultaneous power and data are transferred between multiple transceivers.
3) *Energy efficiency*: no extra power is required by SWIPT-MI for data transfer since the same signal used for power transmission hold the transmitted data. Furthermore, to expand the transmission range, only passive coils could be used for this.
4) *Security*: differently from other wireless communication techniques MI detect easily nodes intrusion and information deformation since data signal modulation is based on the network topology.

The use of MI communications on UWSN through SWIPT could be helpful for building Smart cities, especially in those near water. Many projects are proposed toward this end entitled Smart Water-Smart Cities [148], [149].

## IV. CONCLUSION

EM channel used in terrestrial wireless sensor networks is not suitable for the use in underwater communication due to path losses and dynamic channel conditions. Thus acoustic and MI are mostly used in UWSN. Since they allow good channel quality and reduce the impact of the harsh environmental conditions. Otherwise, some applications cannot use acoustic communication as a wireless channel since they require high throughput and real-time communication. So as MI is recommended for this case mainly for the internet of underwater things, which attract huge interest in these days. Since MI performs in near-field and requires some enhancement to extend its transmission range. Some solutions, as wave-guide, are proposed to deal with this issues. Due to this later, acoustic communication is preferable for applications requiring large transmission range. Wireless power transfer (WPT) is efficiently enabled by the MI, which is useful for UWSN to increase its operating time, which is the primary occupancy of many applications. Contrarily to MI, WPT is not allowed by the acoustic communication. As a perspective, we plan to consider a heterogeneous channel based on the advantages of both acoustic and MI channels. This channel will enable a sophisticated geographic routing for multi-hop data transfer from the bottom to the sea surface station. In this protocol, acoustic communication is used between nodes for low data rate and long communication range. Whereas, MI is used between the underwater nodes considered as a gateway and the sea surface station for high data rate and short communication range.

## REFERENCES

[1] J. G. Proakis, E. M. Sozer, J. A. Rice, and M. Stojanovic. Shallow water acoustic networks. IEEE Communications Magazine, 39(11):114–119, Nov 2001.
[2] Tommaso Melodia, Hovannes Kulhandjian, Li-Chung Kuo, and Emrecan Demirors. Advances in Underwater Acoustic Networking, chapter 23, pages 804–852. John Wiley Sons, Ltd, 2013.
[3] Burhan Gulbahar. Network topology modulation for energy and data transmission in internet of magneto-inductive things. In 2016 IEEE Globecom Workshops (GC Wkshps), pages 1–6, 2016.
[4] A. Kulkarni, V. Kumar, and S. B. Dhok. Enabling technologies for range enhancement of mi based wireless non-conventional media communication. In 2018 9th International Conference on Computing, Communication and Networking Technologies (ICCCNT), pages 1–7, July 2018.
[5] B. Gulbahar. A communication theoretical analysis of multiple-access channel capacity in magneto-inductive wireless networks. IEEE Transactions on Communications, 65(6):2594–2607, June 2017.
[6] E. Liou, C. Kao, C. Chang, Y. Lin, and C. Huang. Internet of underwater things: Challenges and routing protocols. In 2018 IEEE International Conference on Applied System Invention (ICASI), pages 1171–1174, April 2018.
[7] C. Kao, Y. Lin, G. Wu, and C. Huang. A study of applications, challenges, and channel models on the internet of underwater things. In 2017 International Conference on Applied System Innovation (ICASI), pages 1375–1378, May 2017.
[8] M. C. Vuran, A. Salam, R. Wong, and S. Irmak. Internet of underground things: Sensing and communications on the field for precision agricul-

This article has been accepted for publication in a future issue of this journal, but has not been fully edited. Content may change prior to final publication. Citation information: DOI 10.1109/ACCESS.2019.2928876, IEEE Access



ture. In 2018 IEEE 4th World Forum on Internet of Things (WF-IoT), pages 586–591, Feb 2018.

[9] Rodolfo W. L. Coutinho, Azzedine Boukerche, Luiz F. M. Vieira, and Antonio A. F. Loureiro. Underwater wireless sensor networks: A new challenge for topology control-based systems. ACM Comput. Surv., 51(1):19:1–19:36, January 2018.

[10] Seongwon Han, Roy Chen, Youngtae Noh, and Mario Gerla. Real-time video streaming from mobile underwater sensors. In Proceedings of the International Conference on Underwater Networks & Systems, WUWNET '14, pages 21:1–21:8, New York, NY, USA, 2014. ACM.

[11] Seongwon Han, Youngtae Noh, Uichin Lee, and Mario Gerla. Optical-acoustic hybrid network toward real-time video streaming for mobile underwater sensors. Ad Hoc Networks, 83:1 – 7, 2019.

[12] Mari Carmen Domingo. An overview of the internet of underwater things. J. Network and Computer Applications, 35:1879–1890, 2012.

[13] Mari Carmen Domingo. Magnetic induction for underwater wireless communication networks. IEEE Transactions on Antennas and Propagation, 60(6):2929–2939, 2012.

[14] H. Guo, Z. Sun, and P. Wang. Multiple frequency band channel modeling and analysis for magnetic induction communication in practical underwater environments. IEEE Transactions on Vehicular Technology, 66(8):6619–6632, Aug 2017.

[15] S. Kisseleff, I. F. Akyildiz, and W. H. Gerstacker. Survey on advances in magnetic induction-based wireless underground sensor networks. IEEE Internet of Things Journal, 5(6):4843–4856, Dec 2018.

[16] D. N. Sandeep and V. Kumar. Review on clustering, coverage and connectivity in underwater wireless sensor networks: A communication techniques perspective. IEEE Access, 5:11176–11199, 2017.

[17] Mari Carmen Domingo. Overview of channel models for underwater wireless communication networks. Physical Communication, 1(3):163–182, 2008.

[18] Milica Stojanovic. On the relationship between capacity and distance in an underwater acoustic communication channel. In Underwater Networks, 2006.

[19] Milica Stojanovic and James C. Preisig. Underwater acoustic communication channels: Propagation models and statistical characterization. IEEE Communications Magazine, 47:84–89, 2009.

[20] Milica Stojanovic. Underwater acoustic communications: Design considerations on the physical layer. In 2008 Fifth Annual Conference on Wireless on Demand Network Systems and Services, pages 1–10, 2008.

[21] Francisco J. Cañete, Jesús López-Fernández, Celia García-Corrales, Antonio Sánchez, Encarnación Robles, Francisco J. Rodrigo, and Jose Francisco Paris. Measurement and modeling of narrowband channels for ultrasonic underwater communications. In Sensors, 2016.

[22] Junfeng Xu, Keqiu Li, and Geyong Min. Asymmetric multi-path division communications in underwater acoustic networks with fading channels. Journal of Computer and System Sciences, 79(2):269–278, 2013.

[23] Jean-Francois Bousquet, G. McIntyre, and J. Quirion. Time-variant acoustic propagation characterization in seaport deployments. 2015 IEEE 28th Canadian Conference on Electrical and Computer Engineering (CCECE), pages 1520–1525, 2015.

[24] Yinming Cui, Juan Qing, Quansheng Guan, Fei Ji, and Gang Wei. Stochastically optimized fountain-based transmissions over underwater acoustic channels. IEEE Transactions on Vehicular Technology, 64:2108–2112, 2015.

[25] E. M. Sozer, J. G. Proakis, and F. Blackmon. Iterative equalization and decoding techniques for shallow water acoustic channels. In MTS/IEEE Oceans 2001. An Ocean Odyssey. Conference Proceedings (IEEE Cat. No.01CH37295), volume 4, pages 2201–2208 vol.4, Nov 2001.

[26] F. Blackmon, E. Sozer, and J. Proakis. Iterative equalization, decoding, and soft diversity combining for underwater acoustic channels. In OCEANS '02 MTS/IEEE, volume 4, pages 2425–2428 vol.4, Oct 2002.

[27] H. M. Roudsari, J. Bousquet, and G. McIntyre. Channel model for wideband time-varying underwater acoustic systems. In OCEANS 2017 - Aberdeen, pages 1–7, June 2017.

[28] E. Baktash, M. J. Dehghani, M. R. F. Nasab, and M. Karimi. Shallow water acoustic channel modeling based on analytical second order statistics for moving transmitter/receiver. IEEE Transactions on Signal Processing, 63(10):2533–2545, May 2015.

[29] P. A. van Walree and R. Otnes. Ultrawideband underwater acoustic communication channels. IEEE Journal of Oceanic Engineering, 38(4):678–688, Oct 2013.

[30] P. A. van Walree. Propagation and scattering effects in underwater acoustic communication channels. IEEE Journal of Oceanic Engineering, 38(4):614–631, Oct 2013.

[31] James Preisig. Acoustic propagation considerations for underwater acoustic communications network development. SIGMOBILE Mob. Comput. Commun. Rev., 11(4):2–10, October 2007.

[32] M. Naderi, M. Pätzold, and A. G. Zajic. A geometry-based channel model for shallow underwater acoustic channels under rough surface and bottom scattering conditions. In 2014 IEEE Fifth International Conference on Communications and Electronics (ICCE), pages 112–117, July 2014.

[33] M. Naderi, M. Pätzold, R. Hicheri, and N. Youssef. A geometry-based underwater acoustic channel model allowing for sloped ocean bottom conditions. IEEE Transactions on Wireless Communications, 16(4):2394–2408, April 2017.

[34] K. Saraswathi, S. Ravishankar, and R. C. V. Singh. Underwater communications in the presence of bubbles and doppler shift. In 2017 International Conference on Advances in Computing, Communications and Informatics (ICACCI), pages 2173–2179, Sep. 2017.

[35] C. A. Boyles, A. P. Rosenberg, and Q. Zhang. Modeling the effect of bubble plumes on high frequency acoustic propagation in shallow water. In 2013 OCEANS - San Diego, pages 1–8, Sep. 2013.

[36] J. C. Novarini, R. S. Keiffer, and G. V. Norton. A model for variations in the range and depth dependence of the sound speed and attenuation induced by bubble clouds under wind-driven sea surfaces. IEEE Journal of Oceanic Engineering, 23(4):423–438, Oct 1998.

[37] Guy V. Norton and Jorge C. Novarini. On the relative role of sea-surface roughness and bubble plumes in shallow-water propagation in the low-kilohertz region. Journal of the Acoustical Society of America, 110(6):2946–2955, 2001.

[38] C. A. Boyles, A. P. Rosenberg, and Q. Zhang. Underwater acoustic communication channel characterization in the presence of bubbles and rough sea surfaces. In OCEANS 2011 IEEE - Spain, pages 1–8, June 2011.

[39] Peter H. Dahl, Jee Woong Choi, Neil J. Williams, and Hans C. Graber. Field measurements and modeling of attenuation from near-surface bubbles for frequencies 1-20 khz. The Journal of the Acoustical Society of America, 124 3:EL163–9, 2008.

[40] H. S. Dol, M. E. G. D. Colin, M. A. Ainslie, P. A. van Walree, and J. Janmaat. Simulation of an underwater acoustic communication channel characterized by wind-generated surface waves and bubbles. IEEE Journal of Oceanic Engineering, 38(4):642–654, Oct 2013.

[41] Robbert van Vossen and Michael A. Ainslie. The effect of wind-generated bubbles on sea-surface backscattering at 940 hz. The Journal of the Acoustical Society of America, 130 5:3413–20, 2011.

[42] Xingbin Tu, Liangliang Yang, Zhiwen Shao, Zhengrong Zhouwei, and Xiaomei Xu. Study on the impact of bubble curtain on underwater acoustic communication. OCEANS 2014 - TAIPEI, pages 1–5, 2014.

[43] Gabriel Chua, Mandar A. Chitre, and Grant B. Deane. Impact of persistent bubbles on underwater acoustic communication. 2018 Fourth Underwater Communications and Networking Conference (UComms), pages 1–5, 2018.

[44] Grant B. Deane, James C. Preisig, and Andone C. Lavery. The suspension of large bubbles near the sea surface by turbulence and their role in absorbing forward-scattered sound. IEEE Journal of Oceanic Engineering, 38:632–641, 2013.

[45] F. Qu, Z. Wang, L. Yang, and Z. Wu. A journey toward modeling and resolving doppler in underwater acoustic communications. IEEE Communications Magazine, 54(2):49–55, February 2016.

[46] J. S. Dhanoa and R. F. Ormondroyd. Combined differential doppler and time delay compensation for an underwater acoustic communication system. In OCEANS '02 MTS/IEEE, volume 1, pages 581–587 vol.1, Oct 2002.

[47] C. Liu, Y. V. Zakharov, and T. Chen. Doubly selective underwater acoustic channel model for a moving transmitter/receiver. IEEE Transactions on Vehicular Technology, 61(3):938–950, March 2012.

[48] J. Li, Y. V. Zakharov, and B. Henson. Multibranch autocorrelation method for doppler estimation in underwater acoustic channels. IEEE Journal of Oceanic Engineering, 43(4):1099–1113, Oct 2018.

[49] J. Trubuil and T. Chonavel. Accurate doppler estimation for underwater acoustic communications. In 2012 Oceans - Yeosu, pages 1–5, May 2012.

[50] Jingxin Xu, Deqing Wang, Xiaoyi Hu, and Yongjun Xie. Doppler effect mitigation over mobile underwater acoustic ofdm system. In WUWNet, 2018.

[51] Z. Chen, Y. R. Zheng, J. Wang, and J. Song. Synchronization and doppler scale estimation with dual pn padding tds-ofdm for underwater acoustic communication. In 2013 OCEANS - San Diego, pages 1–4, Sep. 2013.

[52] Y. Li, Y. Wang, and X. Guan. Joint synchronization and doppler scale estimation using zadoff-chu sequences for underwater acoustic communications. In OCEANS 2017 - Anchorage, pages 1–5, Sep. 2017.

[53] K. Wang, S. Chen, C. Liu, Y. Liu, and Y. Xu. Doppler estimation and timing synchronization of underwater acoustic communication based on hyperbolic frequency modulation signal. In 2015 IEEE 12th International Conference on Networking, Sensing and Control, pages 75–80, April 2015.

[54] Q. Khuong Nguyen, D. Hung Do, and V. Duc Nguyen. Doppler compensation method using carrier frequency pilot for ofdm-based underwater acoustic communication systems. In 2017 International Conference on Advanced Technologies for Communications (ATC), pages 254–259, Oct 2017.

[55] Shuxia Huang, Shiliang Fang, and Ning Han. An improved velocity estimation method for wideband multi-highlight target echoes in active sonar systems. In Sensors, 2018.

[56] D. V. Ha, V. D. Nguyen, and Q. K. Nguyen. Modeling of doppler power spectrum for underwater acoustic channels. Journal of Communications and Networks, 19(3):270–281, 2017.

[57] Habib Roudsari Mirhedayati and Jean-Francois Bousquet. A time-varying filter for doppler compensation applied to underwater acoustic ofdm. In Sensors, 2018.

[58] Zhaohui Wang, Shengli Zhou, T. C. C. Yang, and Zhijie Jerry Shi. Performance comparison of doppler scale estimation methods for underwater acoustic ofdm. J. Electrical and Computer Engineering, 2012:703243:1–703243:11, 2012.

[59] F. Traverso, T. Gaggero, E. Rizzuto, and A. Trucco. Spectral analysis of the underwater acoustic noise radiated by ships with controllable pitch propellers. In OCEANS 2015 - Genova, pages 1–6, May 2015.

[60] M. Barbeau, S. Blouin, G. Cervera, J. Garcia-Alfaro, B. Hasannezhad, and E. Kranakis. Simulation of underwater communications with a colored noise approximation and mobility. In 2015 IEEE 28th Canadian Conference on Electrical and Computer Engineering (CCECE), pages 1532–1537, May 2015.

[61] Peter H. Dahl, James H. Miller, Douglas H. Cato, and Rex K. Andrew. Underwater ambient noise. Acoustics Today, 3(1):23, 2007.

[62] S. Banerjee and M. Agrawal. On the performance of underwater communication system in noise with gaussian mixture statistics. In 2014 Twentieth National Conference on Communications (NCC), pages 1–6, Feb 2014.

[63] A. Z. Sha'ameri, Y. Y. Al-Aboosi, and N. H. H. Khamis. Underwater acoustic noise characteristics of shallow water in tropical seas. In 2014 International Conference on Computer and Communication Engineering, pages 80–83, Sep. 2014.

[64] National Research Council. Ocean Noise and Marine Mammals. The National Academies Press, Washington, DC, 2003.

[65] M. Rahmati and D. Pompili. Unisec: Inspection, separation, and classification of underwater acoustic noise point sources. IEEE Journal of Oceanic Engineering, 43(3):777–791, July 2018.

[66] F. de Souza, R. Souza, G. Brante, M. Pellenz, F. Rosas, and B. Chang. Code rate optimization for energy efficient delay constrained underwater acoustic communications. In OCEANS 2015 - Genova, pages 1–4, May 2015.

[67] P. Ponnavaikko, K. Yassin, S. K. Wilson, M. Stojanovic, and J. Holliday. Energy optimization with delay constraints in underwater acoustic networks. In 2013 IEEE Global Communications Conference (GLOBECOM), pages 551–556, Dec 2013.

[68] Huseyin Ugur Yildiz. Investigation of maximum lifetime and minimum delay trade-off in underwater sensor networks. International Journal of Communication Systems, 0(0):e3924. e3924 dac.3924.

[69] F. A. de Souza, B. S. Chang, G. Brante, R. D. Souza, M. E. Pellenz, and F. Rosas. Optimizing the number of hops and retransmissions for energy efficient multi-hop underwater acoustic communications. IEEE Sensors Journal, 16(10):3927–3938, May 2016.

[70] Parastoo Qarabaqi and Milica Stojanovic. Acoustic channel simulator, 2013.

[71] Zhiping Wan, Shaojiang Liu, Weichuan Ni, and Zhiming Xu. An energy-efficient multi-level adaptive clustering routing algorithm for underwater wireless sensor networks. Cluster Computing, Mar 2018.

[72] Deqing Wang, Ru Xu, and Xiaoyi Hu. Energy-efficient data aggregation scheme for underwater acoustic sensor networks. In WUWNet, 2015.

[73] Hongpeng Yin, Jinxing Li, Yi Chai, and Simon X. Yang. A survey on distributed compressed sensing: theory and applications. Frontiers of Computer Science, 8:893–904, 2014.

[74] N. Javaid, S. Cheema, M. Akbar, N. Alrajeh, M. S. Alabed, and N. Guizani. Balanced energy consumption based adaptive routing for iot enabling underwater wsns. IEEE Access, 5:10040–10051, 2017.

[75] H. Yang, Y. Zhou, Y. Hu, B. Wang, and S. Kung. Cross-layer design for network lifetime maximization in underwater wireless sensor networks. In 2018 IEEE International Conference on Communications (ICC), pages 1–6, May 2018.

[76] L. Jing, C. He, J. Huang, and Z. Ding. Energy management and power allocation for underwater acoustic sensor network. IEEE Sensors Journal, 17(19):6451–6462, Oct 2017.

[77] Jalaja Janardanan Kartha and Lillykutty Jacob. Network lifetime-aware data collection in underwater sensor networks for delay-tolerant applications. Sādhanā, 42(10):1645–1664, Oct 2017.

[78] Shalli Rani, Syed Hassan Ahmed, Jyoteesh Malhotra, and Rajneesh Talwar. Energy efficient chain based routing protocol for underwater wireless sensor networks. Journal of Network and Computer Applications, 92:42 – 50, 2017. Underwater Acoustic Sensor Networks: Emerging trendsand current perspectives.

[79] F. Bouabdallah, C. Zidi, and R. Boutaba. Joint routing and energy management in underwater acoustic sensor networks. IEEE Transactions on Network and Service Management, 14(2):456–471, June 2017.

[80] J. J. Kartha, A. Jabbar, A. Baburaj, and L. Jacob. Maximum lifetime routing in underwater sensor networks using mobile sink for delay-tolerant applications. In TENCON 2015 - 2015 IEEE Region 10 Conference, pages 1–6, Nov 2015.

[81] Zhong Zhou, Jun-Hong Cui, and Shengli Zhou. Localization for large-scale underwater sensor networks. In Proceedings of the 6th International IFIP-TC6 Conference on Ad Hoc and Sensor Networks, Wireless Networks, Next Generation Internet, NETWORKING'07, pages 108–119, Berlin, Heidelberg, 2007. Springer-Verlag.

[82] Z. Zhou, J. . Cui, and A. Bagtzoglou. Scalable localization with mobility prediction for underwater sensor networks. In IEEE INFOCOM 2008 - The 27th Conference on Computer Communications, pages 2198–2206, April 2008.

[83] T. C. Austin, R. P. Stokey, and K. M. Sharp. Paradigm: a buoy-based system for auv navigation and tracking. In OCEANS 2000 MTS/IEEE Conference and Exhibition. Conference Proceedings (Cat. No.00CH37158), volume 2, pages 935–938 vol.2, Sep. 2000.

[84] R. Thiago Silva da Rosa, G. B. Zaffari, P. J. Dias de Oliveira Evald, P. L. Jorge Drews, and S. Silva da Costa Botelho. Towards comparison of kalman filter methods for localisation in underwater environments. In 2017 Latin American Robotics Symposium (LARS) and 2017 Brazilian Symposium on Robotics (SBR), pages 1–6, Nov 2017.

[85] C. Zheng, D. Sun, L. Cai, and X. Li. Mobile node localization in underwater wireless networks. IEEE Access, 6:17232–17244, 2018.

[86] S. Abougamila, M. Elmorsy, and E. S. Elmallah. A factoring algorithm for probabilistic localization in underwater sensor networks. In 2017 IEEE International Conference on Communications (ICC), pages 1–7, May 2017.

[87] S. Abougamila, M. Elmorsy, and E. S. Elmallah. A graph theoretic approach to localization under uncertainty. In 2018 IEEE International Conference on Communications (ICC), pages 1–7, May 2018.

[88] Sungryul Kim and Younghwan Yoo. Impact of mac delay on auv localization: Underwater localization based on hyperbolic frequency modulation signal. In Sensors, 2018.

[89] Huai Huang and Yahong Rosa Zheng. Node localization with aoa assistance in multi-hop underwater sensor networks. Ad Hoc Networks, 78:32 – 41, 2018.

[90] Jing-Jie Gao, Xiaohong Shen, Ruiqin Zhao, Haodi Mei, and Haiyan Wang. A double rate localization algorithm with one anchor for multi-hop underwater acoustic networks. In Sensors, 2017.

[91] Junhai Luo, Liying Fan, Shan Wu, and Xueting Yan. Research on localization algorithms based on acoustic communication for underwater sensor networks. In Sensors, 2018.

[92] E. Dubrovinskaya, R. Diamant, and P. Casari. Anchorless underwater acoustic localization. In 2017 14th Workshop on Positioning, Navigation and Communications (WPNC), pages 1–6, Oct 2017.

[93] Archana Toky, Rishi Pal Singh, and Sanjoy Das. Coarse-grain localization in underwater acoustic wireless sensor networks. In Ganesh Chandra Deka, Omprakash Kaiwartya, Pooja Vashisth, and Priyanka Rathee,

editors, Applications of Computing and Communication Technologies, pages 187–196, Singapore, 2018. Springer Singapore.

[94] X. M. Tan, Zhi Sun, and Ian F. Akyildiz. Wireless underground sensor networks: Mi-based communication systems for underground applications. IEEE Antennas and Propagation Magazine, 57:74–87, 2015.

[95] Agnelo R. Silva and Mahta Moghaddam. Design and implementation of low-power and mid-range magnetic-induction-based wireless underground sensor networks. IEEE Transactions on Instrumentation and Measurement, 65:821–835, 2016.

[96] Traian E. Abrudan, Orfeas Kypris, Agathoniki Trigoni, and Andrew Markham. Impact of rocks and minerals on underground magneto-inductive communication and localization. IEEE Access, 4:3999–4010, 2016.

[97] Shih-Chun Lin, Abdallah A. Alshehri, Pu Patrick Wang, and Ian F. Akyildiz. Magnetic induction-based localization in randomly deployed wireless underground sensor networks. IEEE Internet of Things Journal, 4:1454–1465, 2017.

[98] Ian F. Akyildiz, Zhi Sun, and Mehmet C. Vuran. Signal propagation techniques for wireless underground communication networks. Physical Communication, 2(3):167 – 183, 2009.

[99] Zhen Zhao, Shuzhi Sam Ge, Wei He, and Yoo Sang Choo. Modeling and simulation of magnetic induction wireless communication for a deepwater mooring system. 2012 IEEE International Conference on Information and Automation, pages 373–378, 2012.

[100] S. Kisseleff, I. F. Akyildiz, and W. H. Gerstacker. Throughput of the magnetic induction based wireless underground sensor networks: Key optimization techniques. IEEE Transactions on Communications, 62(12):4426–4439, Dec 2014.

[101] J.J. Sojdehei, P.N. Wrathall, and D.F. Dinn. Magneto-inductive (mi) communications. In MTS/IEEE Oceans 2001. An Ocean Odyssey. Conference Proceedings (IEEE Cat. No.01CH37295), volume 1, pages 513–519, 2001.

[102] X. Tan, Z. Sun, and I. F. Akyildiz. Wireless underground sensor networks: Mi-based communication systems for underground applications. IEEE Antennas and Propagation Magazine, 57(4):74–87, Aug 2015.

[103] Mehmet C. Vuran, Abdul Salam, Rigoberto Wong, and Suat Irmak. Internet of underground things in precision agriculture: Architecture and technology aspects. Ad Hoc Networks, 81:160 – 173, 2018.

[104] I. F. Akyildiz, P. Wang, and Z. Sun. Realizing underwater communication through magnetic induction. IEEE Communications Magazine, 53(11):42–48, November 2015.

[105] S. Kisseleff, X. Chen, I. F. Akyildiz, and W. Gerstacker. Localization of a silent target node in magnetic induction based wireless underground sensor networks. In 2017 IEEE International Conference on Communications (ICC), pages 1–7, May 2017.

[106] X. Tan and Z. Sun. Environment-aware indoor localization using magnetic induction. In 2015 IEEE Global Communications Conference (GLOBECOM), pages 1–6, Dec 2015.

[107] X. Tan, Z. Sun, and P. Wang. On localization for magnetic induction-based wireless sensor networks in pipeline environments. In 2015 IEEE International Conference on Communications (ICC), pages 2780–2785, June 2015.

[108] Ningcheng Gaoding and Jean-François Bousquet. A compact magneto-inductive coil antenna design for underwater communications. In Proceedings of the International Conference on Underwater and Networks Systems, page 19, 2017.

[109] A. R. Silva and M. Moghaddam. Operating frequency selection for low-power magnetic induction-based wireless underground sensor networks. In 2015 IEEE Sensors Applications Symposium (SAS), pages 1–6, April 2015.

[110] H. Guo and Z. Sun. Increasing the capacity of magnetic induction communication using mimo coil-array. In 2016 IEEE Global Communications Conference (GLOBECOM), pages 1–6, Dec 2016.

[111] Z. Sun, I. F. Akyildiz, S. Kisseleff, and W. Gerstacker. Increasing the capacity of magnetic induction communications in rf-challenged environments. IEEE Transactions on Communications, 61(9):3943–3952, Sep. 2013.

[112] L. Erdogan and J. . Bousquet. Dynamic bandwidth extension of coil for underwater magneto-inductive communication. In 2014 IEEE Antennas and Propagation Society International Symposium (APSURSI), pages 1576–1577, July 2014.

[113] Z. Zhang, E. Liu, X. Qu, R. Wang, H. Ma, and Z. Sun. Connectivity of magnetic induction-based ad hoc networks. IEEE Transactions on Wireless Communications, 16(7):4181–4191, July 2017.

[114] A. R. Silva and M. Moghaddam. Strategic frequency adaptation for mid-range magnetic induction-based wireless underground sensor networks. In 2015 Annual IEEE Systems Conference (SysCon) Proceedings, pages 758–765, April 2015.

[115] Burhan Gulbahar and Ozgur B. Akan. A communication theoretical modeling and analysis of underwater magneto-inductive wireless channels. IEEE Transactions on Wireless Communications, 11(9):3326–3334, 2012.

[116] Hongzhi Guo, Zhi Sun, and Pu Wang. Channel modeling of mi underwater communication using tri-directional coil antenna. 2015 IEEE Global Communications Conference (GLOBECOM), pages 1–6, 2014.

[117] R. R.A. Syms, E. Shamonina, and L. Solymar. Positive and negative refraction of magnetoinductive waves in two dimensions. European Physical Journal B, 46(2):301–308, 2005.

[118] Niaz Ahmed, Justin Hoyt, Andriy Radchenko, David Pommerenke, and Y. Rosa Zheng. A multi-coil magneto-inductive transceiver for low-cost wireless sensor networks. 2014 Underwater Communications and Networking (UComms), pages 1–5, 2014.

[119] Jiaxin Zhou and Jianyong Chen. Maximum distance estimation of far-field model for underwater magnetic field communication. 2017 IEEE 7th Annual Computing and Communication Workshop and Conference (CCWC), pages 1–5, 2017.

[120] Yibin Wang, Andrew Dobbin, and Jean-François Bousquet. A compact low-power underwater magneto-inductive modem. In Proceedings of the 11th ACM International Conference on Underwater and Networks Systems, page 14, 2016.

[121] J. I. Agbinya and M. Masihpour. Power equations and capacity performance of magnetic induction body area network nodes. In 2010 Fifth International Conference on Broadband and Biomedical Communications, pages 1–6, 2010.

[122] Hoang Nguyen, Johnson I. Agbinya, and John Devlin. Channel characterisation and link budget of mimo configuration in near field magnetic communication. International Journal of Electronics and Telecommunications, 59(3), 2013.

[123] H. J. Kim, J. Park, K. S. Oh, J. P. Choi, J. E. Jang, and J. W. Choi. Near-field magnetic induction mimo communication using heterogeneous multipole loop antenna array for higher data rate transmission. IEEE Transactions on Antennas and Propagation, 64(5), 2016.

[124] H. J. Kim and J. W. Choi. Crosstalk-free magnetic mimo communication using heterogeneous antenna array. In 2016 URSI Asia-Pacific Radio Science Conference (URSI AP-RASC), pages 1–3, 2016.

[125] Z. Sun and I. F. Akyildiz. Underground wireless communication using magnetic induction. In 2009 IEEE International Conference on Communications, pages 1–5, 2009.

[126] Z. Sun and I.F. Akyildiz. Magnetic induction communications for wireless underground sensor networks. IEEE Transactions on Antennas and Propagation, 58(7):2426–2435, 2010.

[127] S. Kisseleff, B. Sackenreuter, I. F. Akyildiz, and W. Gerstacker. On capacity of active relaying in magnetic induction based wireless underground sensor networks. In 2015 IEEE International Conference on Communications (ICC), pages 6541–6546, 2015.

[128] M. Masihpour, D. R. Franklin, and M. Abolhasan. Multihop relay techniques for communication range extension in near-field magnetic induction communication systems. JNW, 8(5):999–1011, 2013.

[129] N. Ahmed, Y. R. Zheng, and D. Pommerenke. Theoretical modeling of multi-coil channels in near field magneto-inductive communication. In 2015 IEEE 82nd Vehicular Technology Conference (VTC2015-Fall), pages 1–5, 2015.

[130] Hongzhi Guo, Zhi Sun, Jingbo Sun, and Natalia M Litchinitser. $M^2I$: Channel modeling for metamaterial-enhanced magnetic induction communications. IEEE Transactions on Antennas and Propagation, 63:5072–5087, 2015.

[131] H. Guo and Z. Sun. $M^2I$ communication: From theoretical modeling to practical design. In 2016 IEEE International Conference on Communications (ICC), pages 1–6, May 2016.

[132] Zhi Sun and Hongzhi Guo. Demo abstract: Prototyping $M^2I$ communication system for underground and underwater networks. 2017 IEEE Conference on Computer Communications Workshops (INFOCOM WKSHPS), pages 962–963, 2017.

[133] Hongzhi Guo, Zhi Sun, and Chi Zhou. Practical design and implementation of metamaterial-enhanced magnetic induction communication. IEEE Access, 5:17213–17229, 2017.

[134] Priya Kumari Sharma, Deepak Bhatia, and R. S. Meena. Metamaterial enhanced magnetization induced communication for wireless applica-

tions. 2017 International Conference on Information, Communication, Instrumentation and Control (ICICIC), pages 1–5, 2017.

[135] Agnelo R. Silva and Majid Moghaddam. Strategic frequency adaptation for mid-range magnetic induction-based wireless underground sensor networks. 2015 Annual IEEE Systems Conference (SysCon) Proceedings, pages 758–765, 2015.

[136] Xin Tan and Zhi Sun. On environment-aware channel estimation for wireless sensor networks using magnetic induction. 2017 IEEE Conference on Computer Communications Workshops (INFOCOM WKSHPS), pages 217–222, 2017.

[137] Steven Kisseleff, Ian F. Akyildiz, and Wolfgang H. Gerstacker. Beamforming for magnetic induction based wireless power transfer systems with multiple receivers. 2015 IEEE Global Communications Conference (GLOBECOM), pages 1–7, 2014.

[138] Mohammad R. Vedady Moghadam and Rui Zhang. Node placement and distributed magnetic beamforming optimization for wireless power transfer. IEEE Transactions on Signal and Information Processing over Networks, 4:264–279, 2018.

[139] Nikolay Tal, Yahav Morag, and Yoash Levron. Design of magnetic transmitters with efficient reactive power utilization for inductive communication and wireless power transfer. 2015 IEEE International Conference on Microwaves, Communications, Antennas and Electronic Systems (COMCAS), pages 1–5, 2015.

[140] Steven Kisseleff, Ian F. Akyildiz, and Wolfgang H. Gerstacker. Magnetic induction-based simultaneous wireless information and power transfer for single information and multiple power receivers. IEEE Transactions on Communications, 65:1396–1410, 2017.

[141] Sun-Hee Kim, Yong-Seok Lim, and Seung-Jun Lee. Magnetic resonant coupling based wireless power transfer system with in-band communication. Journal of Semiconductor Technology and Science, 13(6):562–568, 2013.

[142] Mohammad R. Vedady Moghadam and Rui Zhang. Multiuser wireless power transfer via magnetic resonant coupling: Performance analysis, charging control, and power region characterization. ieee transactions on signal and information processing over networks, 2(1):72–83, 2016.

[143] Xiaofei Li, Chunsen Tang, Xin Dai, Pengqi Deng, and Yugang Su. An inductive and capacitive combined parallel transmission of power and data for wireless power transfer systems. IEEE Transactions on Power Electronics, 33(6):4980–4991, 2018.

[144] Gang Yang, Mohammad R. Vedady Moghadam, and Rui Zhang. Magnetic beamforming for wireless power transfer. In 2016 IEEE International Conference on Acoustics, Speech and Signal Processing (ICASSP), pages 3936–3940, 2016.

[145] Kyungtae Kim, Han-Joon Kim, and Ji-Woong Choi. Magnetic beamforming with non-coupling coil pattern for high efficiency and long distance wireless power transfer. In 2017 IEEE Wireless Power Transfer Conference (WPTC), pages 1–4, 2017.

[146] J. I. Agbinya and S. Lal. A high capacity near-field inductive coupled miso communication system for internet of things. In 7th International Conference on Broadband Communications and Biomedical Applications, pages 112–117, Nov 2011.

[147] Chien-Chi Kao, Yi-Shan Lin, Geng-De Wu, and Chun-Ju Huang. A comprehensive study on the internet of underwater things: Applications, challenges, and channel models. Sensors, 17(7), 2017.

[148] Avneet Prasad, Kabir Mamun, F M Rabiul Islam, and Haq Haqva. Smart water quality monitoring system. In 2015 2nd Asia-Pacific World Congress on Computer Science and Engineering (APWC on CSE), pages 1–6, 2015.

[149] Leonardo Gabrielli, Mirco Pizzichini, Susanna Spinsante, Stefano Squartini, and Roberto Gavazzi. Smart water grids for smart cities: A sustainable prototype demonstrator. In Networks and Communications (EuCNC), 2014 European Conference on, pages 1–5, 2014.

• • •